Depositional cycles, composite sea-level changes, cycle stacking patterns, and the hierarchy of stratigraphic forcing: Examples from Alpine Triassic platform carbonates

R. K. GOLDHAMMER*
P. A. DUNN
L. A. HARDIE
Department of Earth and Planetary Sciences, Johns Hopkins University, Baltimore, Maryland 21218

ABSTRACT

Carbonate platform deposits record a complex interplay of numerous geodynamic variables, of which eustasy, subsidence, and sediment accumulation are prime factors in determining both the kilometer-scale (depositional sequence scale) and meter-scale (depositional cycle scale) stratigraphic packaging. In this study, we looked particularly at composite eustasy, that is, superimposed sea-level fluctuations with different frequencies (defined as orders) and different amplitudes, and the role it plays in the linkage between meter-scale cyclic stratigraphy and kilometer-scale sequence stratigraphy. Specifically, we have investigated the relationship between low-frequency, third-order (1–10 m.y. period) depositional cycles and their component high-frequency, fourth-(0.1–1 m.y.) and fifth-(0.01–0.1 m.y.) order cycles through detailed stratigraphic analyses of Alpine Triassic platforms, complemented by computer modeling. On the basis of our results, we suggest that in general, there exists a hierarchy of stratigraphic forcing driven by composite eustasy that results in organized stacking patterns (thickness, subfacies character, early diagenetic attributes) of high-frequency, typically fourth- and fifth-order, shallow-water carbonate cycles dictated by low-frequency, third-order relative sea-level effects. We suggest that systematic vertical changes in stacking patterns of high-frequency cycles across a larger depositional sequence are due to systematic and predictable differences in depositional space available during the rising and falling stages of a relative third-order sea-level change. We also suggest that these systematic variations in cycle stacking patterns will exist regardless of the mechanism responsible for generating the high-frequency cycles, be it an autocyclic or allocyclic mechanism. This approach has major implications for the use of high-frequency, fourth- and fifth-order cycle characteristics to identify third-order cycles in outcrops and cores of shallow-water carbonates, where stratigraphic control may be less than desirable. This would constitute a valuable bridge between cyclic stratigraphy at the meter scale and sequence stratigraphy at the seismic scale.

We present two examples from Triassic buildups of the Alps (the Ladinian Latemar buildup and the Norian Dolomia Principale) where a systematic succession of high-frequency cycle stacking patterns and early diagenetic features exists within an overriding third-order cycle (sequence) reflecting the interplay of short-term, high-frequency (fourth, fifth order) eustasy and long-term, low-frequency (third order) eustasy in accordance with the hierarchy of stratigraphic forcing. Central to the interpretation of these examples is the demonstration that true eustatic rhythms are recorded in the high-frequency cyclicity, as verified by time-series analyses and the use of "Fischer plots." These examples can be modeled by computer under conditions of lag-depth–constrained sedimentation, uniform subsidence, and composite eustasy. We also present two examples, one from the Alpine Triassic (the Norian Lofer cyclothems) and one from the Pleistocene of south Florida, that lack both a systematic succession of high-frequency cycle stacking patterns and identifiable composite rhythms in the stratigraphic record, despite the existence of composite high-frequency eustasy. In these examples, we call upon (1) local tectonic forcing in the form of short-term deviations in subsidence via faulting (Lofer example) and (2) large differences in the relative amplitudes of different orders of high-frequency sea-level oscillations (Pleistocene example) to explain the lack of composite rhythms, and we present computer simulations to illustrate the concepts. An understanding of composite relative sea-level changes and the potential for a hierarchy of stratigraphic forcing provides the link between cyclostratigraphy and sequence stratigraphy and also has important implications regarding the stratigraphy of early diagenesis.

INTRODUCTION

The geometry and stratigraphy of shallow-marine carbonate deposits are the result of a complex interplay of eustatic sea-level fluctuations, subsidence, sediment production and accumulation rates, climate, antecedent depositional topography, and compaction effects (see numerous examples in Crevello and others, 1989). Of these variables, eustasy, subsidence, and sedimentation are most critical in controlling the disposition of depositional facies on carbonate platforms (Hardie and Shinn, 1986). Rates of long-term subsidence of passive margins and cratonic basins range from 1 to 25 cm/1,000 yr (Schlager, 1981), and changes in these rates occur slowly and exponentially (Bott, 1982). Carbonate sediment production rates on shallow-marine platforms typically exceed these tectonic subsidence rates (Schlager, 1981), allowing thick successions of shallow-water platform carbonates to accumulate in cratonic basins and on passive margins during drift stages of continental separation. Eustatic sea-level changes, on the other hand, may recur repeatedly at high frequencies (10^4–10^5 yr) and at rapid rates (as much as 10 m/1,000 yr, Schlager, 1981) that can outstrip carbonate production rates. The resulting stratigraphic record is one of cyclic accumulation, with each depositional

*Present address: Exxon Production Research Company, P.O. Box 2189, Houston, Texas 77252-2189.

Geological Society of America Bulletin, v. 102, p. 535–562, 23 figs., May 1990.

cycle in the vertical stack of cycles capped by a nondepositional diastem (Barrell, 1917). Eustatic oscillations in sea level occur with different frequencies, yielding an ordered hierarchy of eustasy based upon the duration of each fluctuation. Significantly, different orders of eustasy have characteristic amplitudes and rates of change (Donovan and Jones, 1979), reflecting the driving mechanism, whether glacio-eustatic (change in the volume of water) or tectono-eustatic (change in the volume of the ocean basins), and these different orders of eustasy may be superimposed to give a complex succession of sea-level oscillations. This concept of composite eustasy (Suess, 1888; Grabau, 1913; Barrell, 1917) is, in our view, critical in evaluating and predicting platform carbonate stratigraphy. In particular, in the evolution of shallow-marine carbonate platform deposits, the combined effects of third-(1–10 m.y.), fourth-(0.1–1 m.y.), and fifth-(0.01–0.1 m.y.) order eustatic cycles, should be of prime importance in determining both the kilometer-scale (depositional sequence scale) and meter-scale (depositional cycle scale) stratigraphic packaging. The connection between composite sea-level changes and stacking patterns of depositional cycles is the focus of the present paper.

The magnificently exposed, kilometer-scale Triassic carbonate platforms of the Southern Alps (Italy) and the Northern Limestone Alps (Austria) are characterized by cyclic sedimentation on a meter scale, as the pioneering studies of Sander (1936), Schwarzacher (1954), Fischer (1964), and Bosellini (1965, 1967) have demonstrated. Our own recent studies of the Middle and Upper Triassic cyclic platform carbonates of the Southern Alps (Bosellini and Hardie, 1985; Hardie and others, 1986; Goldhammer and others, 1987; Goldhammer, 1987; Goldhammer and Harris, 1989) provide very strong evidence that these Triassic cycles were controlled primarily by composite eustatic sea-level changes in the Milankovitch band (10^4–10^5 yr), as Alfred Fischer had suggested in his classic 1964 paper on the Lofer facies of the Dachstein Kalk. The work reported in the present paper is an extension of our earlier studies of the Triassic platform carbonates of the Alps. We have explored the possible consequences of high-frequency composite sea-level changes on cyclic sedimentation on shallow carbonate platforms, with particular emphasis on the vertical stacking patterns of high-frequency cycles, and the fundamental relationship between high-frequency cycles and low-frequency depositional sequences. We present evidence of how regular "beats" of an oscillating Triassic sea level were "caught" or "missed" in the stratigraphic record as a result of the interaction of three different orders of relative sea-level change, that is, third order (1–10 m.y.), fourth order (0.1–1 m.y.), and fifth order (0.01–0.1 m.y.), resulting in a systematic succession of high-frequency stacking patterns. In light of our findings for the Alpine Triassic, we suggest that there exists a hierarchy of stratigraphic forcing driven by composite eustasy, which results in organized stacking patterns (thickness, subfacies character, early diagenetic attributes) of high-frequency, shallow-water carbonate cycles dictated by low-frequency rela-

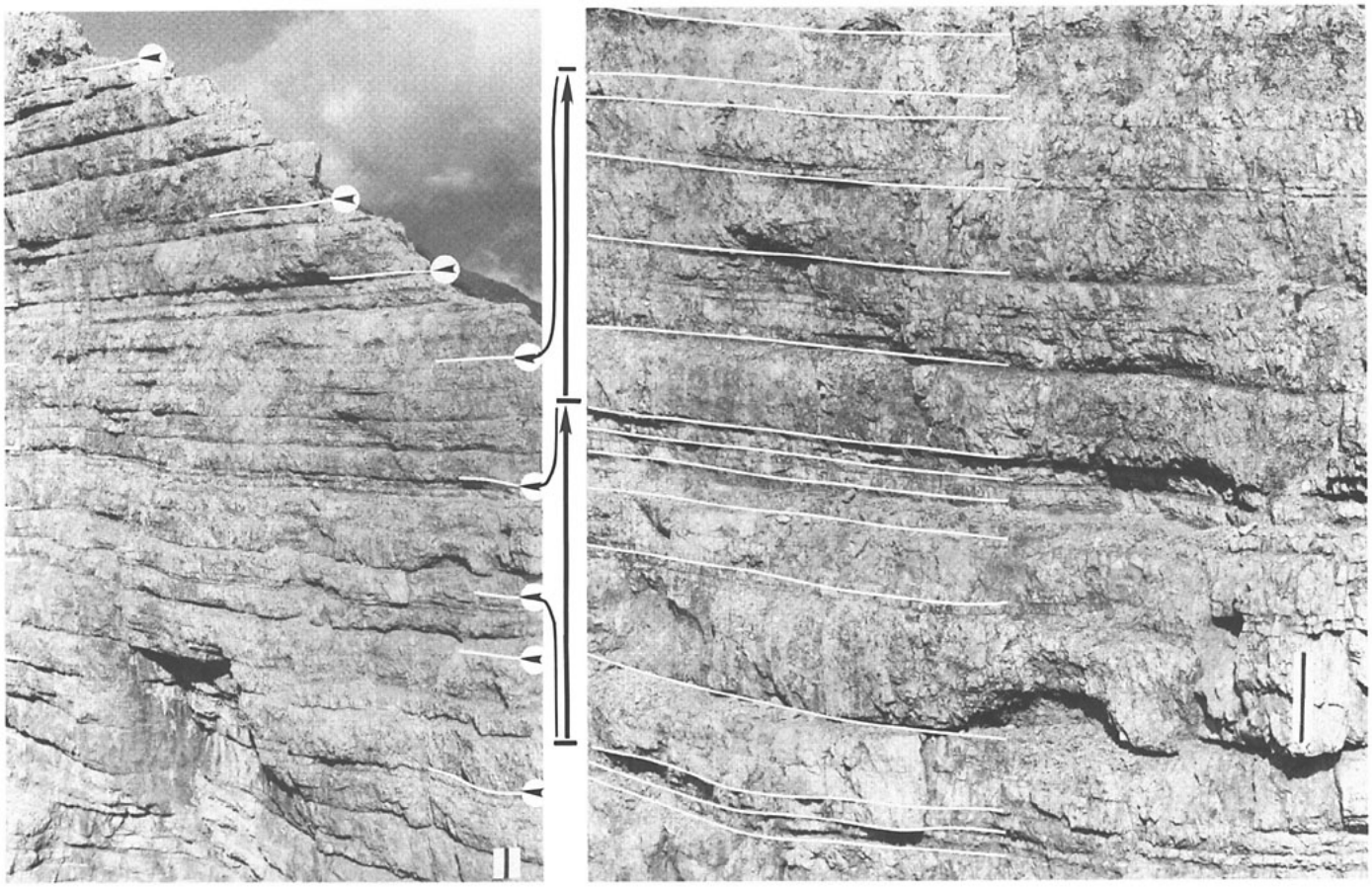

Figure 1. Outcrop photographs of depositional cycles of the upper cyclic facies of the Latemar platform. View at left shows succession of thin beds of limestone separated by vadose diagenetic caps (dark, recessive bands), with arrows marking tops of thinning-upward megacycles. Photograph at right gives detailed view of the megacycles, with individual cycle caps marked and the total number of cycles in each megacycle indicated. Scale bar is 2 m.

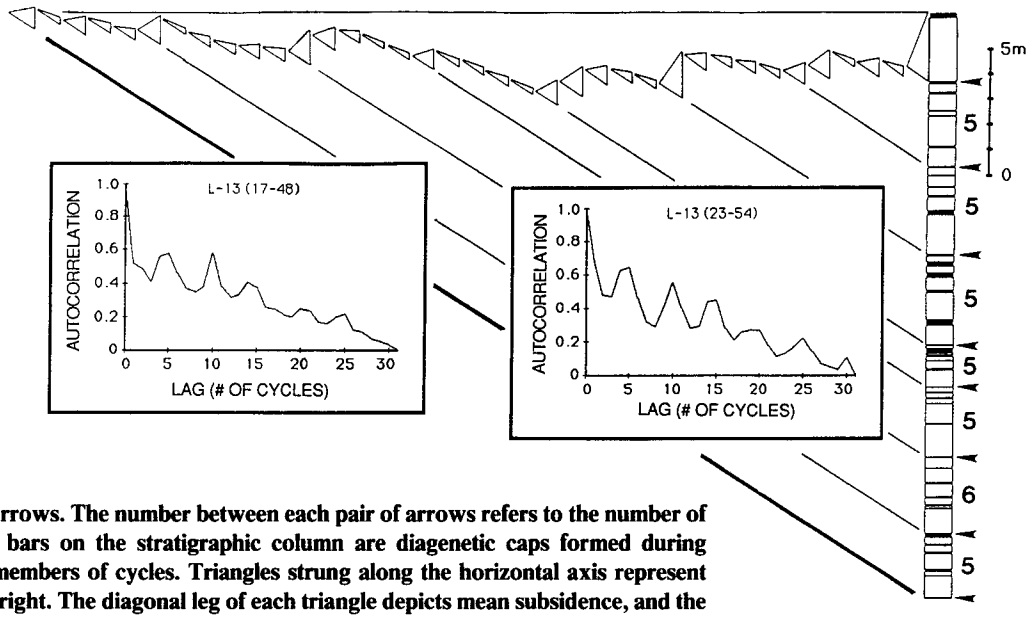

Figure 2. "Fischer diagram" of 37 consecutive meter-scale cycles (measured section L-13, cycles 17–53) from the upper cyclic facies of the Latemar buildup. The vertical column represents a measured stratigraphic section, and the horizontal axis depicts relative time, becoming progressively younger to the right. The heavy diagonal line connecting the base of the stratigraphic section to the initial time point is the mean subsidence vector. The autocorrelation graphs (insets) refer to different but overlapping sets of 32 consecutive cycles. Boundaries between megacycles are indicated on the stratigraphic section by arrows. The number between each pair of arrows refers to the number of cycles within that megacycle. Black bars on the stratigraphic column are diagenetic caps formed during exposure; white represents subtidal members of cycles. Triangles strung along the horizontal axis represent cycles in ascending order from left to right. The diagonal leg of each triangle depicts mean subsidence, and the vertical side depicts cycle thickness. The top of each triangle is the sum of these two vectors. From Goldhammer and others (1987).

tive sea-level changes. We also suggest that these systematic variations in cycle stacking patterns will exist regardless of the mechanism responsible for generating the high-frequency cycles, be it an autocyclic or allocyclic mechanism. This approach has major consequences for the use of high-frequency, fourth- and fifth-order cycle characteristics to identify third-order cycles (equivalent to the sequences of Vail, 1987, and Van Wagoner and others, 1987) in outcrops and cores of shallow-water carbonates, where stratigraphic control is poor. This would constitute a valuable bridge between cyclic stratigraphy at the meter scale and sequence stratigraphy at the seismic scale.

RHYTHMIC AND NONRHYTHMIC SEDIMENTATION: SANDER'S RULE

Central to an understanding of the causes and consequences of high-frequency cyclicity driven by relative sea-level changes is the issue of whether the stratigraphic succession of sedimentary cycles was the result of rhythmic events, such as astronomically forced eustatic oscillations of sea level, or nonrhythmic processes, such as nonuniform subsidence. This general issue of rhythmicity in cyclic deposits was raised by Bruno Sander (1936, 1951), in his pioneering study of the Dachstein (Lofer) and other Triassic carbonates of the Alps, and subsequently elaborated by his student Walter Schwarzacher (1975). Sander (1936), in a classic publication on the Triassic carbonates of the Alps, expressed the view, "we can not conclude from sequences that are non-rhythmic in space that the control has been non-rhythmic in time but we must conclude from sequences that are rhythmic in space that there has been a time-rhythmic control (law of the rhythmic record)" (from the English translation of Sander's 1936 paper, see Sander, 1951, p. 16). Using statistical arguments, Schwarzacher (1975) substantiated Sander's contention that any regular pattern found in the stratigraphic record cannot be the result of random processes but, instead, must be a response to a regular pattern in the time distribution of events. Schwarzacher (1975, p. 288) has called this premise "Sander's Rule" and has presented it as follows: "cyclicity in space (which means stratigraphical thickness) indicates cyclicity in time but the absence of cyclicity in the stratigraphical record does not indicate the absence of time cyclicity."

Schwarzacher (1975) argued further that such a time pattern of events is likely to have been more regular than its record in the stratigraphic column, which because of the complexity of sedimentation processes, is at best a rather "faulty recording mechanism." Thus, nonrhythmic patterns in the stratigraphic record do not necessarily mean that the controlling forces were nonrhythmic. This concept is a fundamental one and underlies our basic approach to the problem of platform carbonate cyclicity.

EVIDENCE FOR RHYTHMIC SEDIMENTATION IN THE TRIASSIC OF THE SOUTHERN ALPS

In the Dolomites region of the Southern Alps in northern Italy, the Anisian-Ladinian carbonate buildup known as the Latemar massif (5–6 km across) consists of a core of flat-lying platform carbonates about 800 m thick encircled by steeply dipping foreslope breccias that grade laterally into basinal deposits (see also Bosellini and Rossi, 1974; Gaetani and others, 1981; Bosellini, 1984; Goldhammer and Harris, 1989). The upper platform is an approximately 400-m-thick stack of about 500 thin cycles of Ladinian age (known as the Latemar Limestone) that carries abundant evidence of repeated subaerial exposure as a result of high-frequency sea-level oscillations (Hardie and others, 1986; Goldhammer and others, 1987; Goldhammer, 1987). Each cycle is a couplet consisting of a basal subtidal skeletal-lithoclast grainstone (0.6–0.7 m average thickness) overlain by a 1- to 15-cm-thick cap of dolomitized grainstone with meniscus and pendant cements, micrite-coated grains, solution-enlarged pores, and other evidence of vadose diagenesis and calichification (Goldhammer and others, 1987, p. 857–869). These couplets are grouped into five-part megacycles (as much as 5 m thick) characterized by progressive upward thinning of successive cycles within each megacycle (Fig. 1). The repetitive bundling of cycles into these five-part megacycles is revealed graphically on Fischer diagrams (Fig. 2) and confirmed by autocorrelative time-series analysis (Fig. 2).

Goldhammer and others (1987) argued that the five-part thinning-upward megacycles of the Ladinian Latemar platform are the result of high-frequency fourth- and fifth-order (10^5 and 10^4 yr duration, respec-

tively) composite sea-level oscillations in tune to Milankovitch astronomical rhythms. Their arguments were based on comparison with the Pleistocene sea-level record and on computer simulation of the Latemar cyclic stratigraphy using Milankovitchian sea-level oscillations. Despite large errors in radiometric dates of the Ladinian stage boundaries (for example, Palmer, 1983), the average duration of an individual cycle must have been on the order of 10^4 yr (8,000 to 20,000 yr) and that of a megacycle must have been on the order of 10^5 yr. Asymmetrical sea-level oscillations with 5-part composite frequencies in this 10^4- to 10^5-yr range were a particular characteristic of the Pleistocene ocean. Dated coral reef terraces and oxygen isotope data from deep-sea sediments have been used to demonstrate that Pleistocene glacio-eustatic sea-level oscillations consisted of a rhythmic series of asymmetric approximately 100,000-yr waves (rate of rise > rate of fall) on which were superimposed 5 higher-order sinusoidal approximately 20,000-yr waves (Fig. 3). Spectral analysis of the oxygen isotope data of the deep-sea sediments has established the case for Milankovitch forcing of this Pleistocene glacio-eustasy (Hays and others, 1976; Imbrie and others, 1984). Using the Pleistocene eustatic sea-level curves as an analogy, Goldhammer and others (1987) were able to quantitatively simulate the Latemar cyclic stratigraphy of five-part megacycles composed of upward-thinning cycles (submeter scale) with thin soil caps (Fig. 4). In these simulations, sedimentation rates, subsidence rates, soil formation rates, and so on, were constrained by values known from Holocene-Pleistocene carbonate depositional systems. These data were combined with sea-level oscillations operating in the Milankovitch composite cycle mode (20,000/100,000-yr scale). On the basis of the Pleistocene comparison and the quantitative simulation, and in the absence of any other known mechanism that could produce 5-part composite sea-level oscillations in the 10^4- to 10^5-yr range, Goldhammer and others (1987) called on Milankovitch-driven eustasy to explain the cyclic stratigraphy of the Triassic Latemar platform carbonates.

Hinnov and Goldhammer (1988) used high-resolution multitaper spectral analysis to scan the cycle thickness data from the Latemar for Milankovitch and other spectral lines. Because of the uncertainties in the age dating of the Ladinian stage boundaries, the analysis was carried out with dimensionless frequencies and the assumption that the cycles were of equal duration. When the resulting spectrum was calibrated with a sampling rate of ~20,000 yr per meter-scale cycle, there emerged a set of statistically significant signals that correspond to within 5% to the 41,000-, 53,000-, 95,000-, and 100,000-yr Milankovitch lines predicted by Berger (1988, Table 3) for the solar insolation variation at the Earth's surface over the past 5 m.y. This correspondence adds considerable weight to the interpretation that the Latemar cyclic series records a regular "beat" of ~100,000 yr (modulating between about 95,000 and 131,000 yr) on which are superimposed five ~20,000-yr "beats" (as shown in Fig. 4).

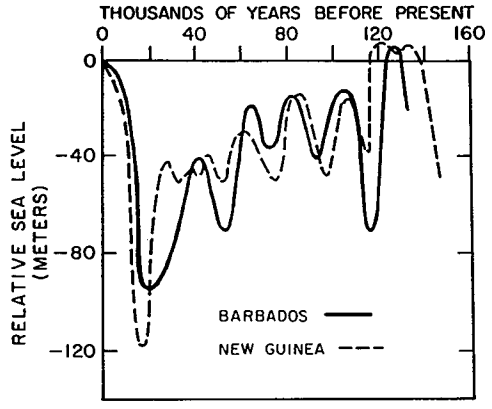

Figure 3. Pleistocene sea-level curves over the past 140,000 yr, constructed from dated coral reef terraces in Barbados and New Guinea, showing approximately 20,000-yr oscillations superimposed on an asymmetric approximately 100,000-yr oscillation. From Goldhammer and others (1987).

This, then, is the case for rhythmic sedimentation during Triassic times. It must be tempered by the fact that without closely spaced and exceedingly accurate age dates it will never be possible to unequivocally demonstrate that a regular stratigraphic succession of sedimentary cycles is a "time cyclic sequence" in which each cycle was formed at equal time intervals (Schwarzacher, 1975, p. 255). Until such time as radiometric dating of the stratigraphic record becomes accurate enough to carry out absolute time-series analyses on cyclic successions, we will have to rely on the common-sense view of Bruno Sander that an ordered stratigraphic succession is not likely to have resulted from a disordered succession of time events (Schwarzacher, 1975, p. 288). As our principal working hypothesis, then, consistent with Sander's Rule, we regard the cyclic facies of the Latemar buildup as rhythmically deposited by a regular sequence of events (rise and fall of sea level) that repeated at equal, or nearly so, time intervals on the order of 20,000 yr. With this interpretation, the individual sedimentary cycles, that is, the individual Latemar couplets bounded by subaerial exposure surfaces, are "deterministic" cycles in the sense of Schwarzacher (1975), each with a fundamental time value of ~20,000 yr. There are some important consequences of this interpretation. The stratigraphic succession of these Triassic cycles, where they follow one another without interruption, becomes in essence a "strip chart recording" of the rhythms of Latemar sedimentation, that is, subaqueous deposition of lime sand alternating with subaerial exposure and vadose diagenesis, all controlled by the rhythmic rises and falls of sea level above and below the flat top of the Latemar platform. Because the fundamental "beat" of these rhythms is presumed to be that of the Milankovitch precessional periodicity, that is, ~20,000 yr, this Latemar "strip chart" may also be a precise record of the time that elapsed during rhythmic growth of the Latemar buildup. There is a minimum of 488 fifth-order cycles in the Ladinian section of the Latemar platform, giving a minimum duration of 9.76 m.y. for the Ladinian stage. This compares reasonably well with duration based on the published radiometric ages for the Ladinian, that is, 10 ± 10 m.y. (Webb, 1981), 7 ± 18 m.y. (Harland and others, 1982), 5 ± 16 m.y. (Palmer, 1983), and 4 ± 9 m.y. (Odin and Letolle, 1982). For a discussion of the possible use of cycles in chronostratigraphy, see House (1985), Fischer (1986), and Schwarzacher (1987). Finally, the regular repetitive pattern of deposition of these cycles in the form of five-part thinning-upward megacycles provides a standard against which other Triassic platform cyclic successions can be tested for rhythmicity, degree of departure from rhythmicity, or lack of rhythmicity. This is explored in some detail in the next section.

CAUGHT AND MISSED BEATS: RHYTHMIC, AMALGAMATED, AND CONDENSED MEGACYCLES

If the Latemar rhythmic sedimentation was the product of astronomically forced rhythmic oscillations of the Triassic ocean, then we should expect to find evidence of these rhythms in other Triassic platform carbonates. As documented below, however, the regular repetition of five-part megacycles displayed by the Latemar succession is exceptional rather than normal in those Triassic cyclic platform deposits we have examined in northern Italy and Austria. In an attempt to find an explanation for the

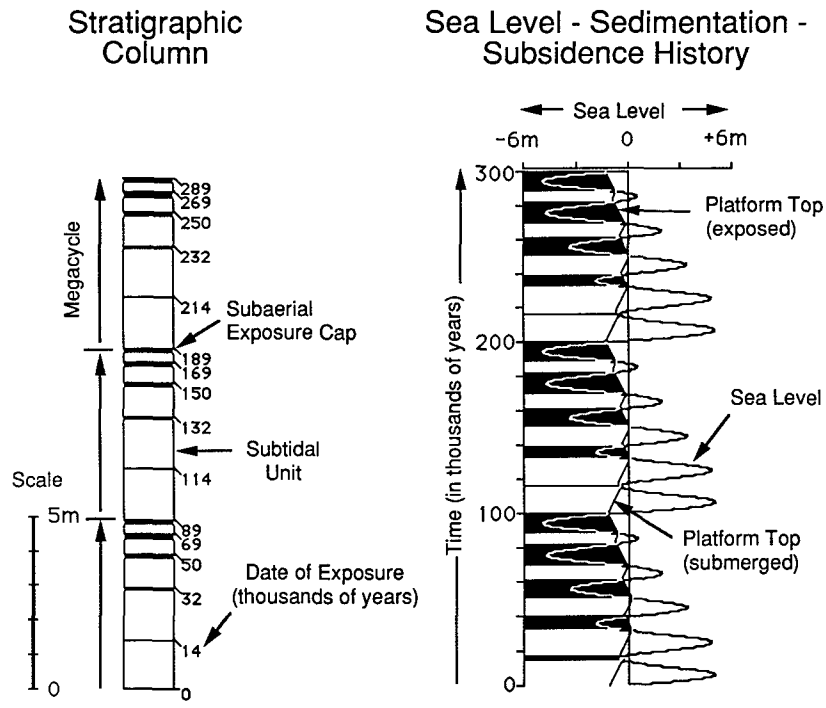

Figure 4. Computer simulation of Latemar platform megacycles. Stratigraphic column (left) shows three complete fourth-order megacycles consisting of 5-m-scale fifth-order cycles composed of subtidal limestone (white) and dolomitic exposure cap (black). Chart (right) illustrates the interaction of composite sea level (asymmetric, 100,000-yr sawtooth wave and superimposed 20,000-yr sinusoidal oscillation) with platform sedimentation and subsidence during the run. See also Goldhammer and others (1987), Figures 15 and 16.

differences among these Alpine Triassic cyclic successions, we have explored the concept, inherent in Sander's Rule, that "equally spaced time events" can be recorded in the stratigraphic column as "unequally spaced lithologic events" (Schwarzacher, 1975, p. 288).

We have investigated the sensitivity of the structure of the five-part megacycles to changes in such parameters as subsidence rate, sedimentation rate, periodicities and amplitudes of the eustatic sea-level oscillations, using our "Mr. Sediment" computer program that was designed to simulate the Latemar cyclic stratigraphy (Dunn and others, 1986; Goldhammer and others, 1987, p. 876–884).

"Mr. Sediment" generated a "Latemar-type" cyclic stratigraphy when a high-frequency (approximately 20,000-yr period) sinusoidal sea-level oscillation was superimposed on top of a lower-frequency (approximately 100,000-yr period) asymmetric pulse. An *asymmetric* 100,000-yr wave was found essential to reproduce the thinning-upward megacycles. With the Pleistocene sea-level curve (Fig. 3) as a guide, we used asymmetrical waves in which the duration of the rise to a maximum occupied between 16% and 30% of the total period (that is, 16,000 to 30,000 yr for a 100,000-yr period); however, here the similarity with the Pleistocene composite eustasy ends because it proved necessary to keep the amplitude of the 100,000-yr wave smaller or equal to that of the 20,000-yr wave in order to simulate the Latemar cyclostratigraphy. The significance of the similarities and differences between the Pleistocene and the Triassic composite eustasy has been discussed by Goldhammer and others (1987, p. 886). The "Mr. Sediment" program generated cycles by oscillating sea level above a constantly subsiding base level, with sediment aggrading vertically until the sediment surface is intersected by sea level. At that point, subtidal sedimentation ceases and if sea level continues to drop below the top of the sediment column (that is, the platform top), subaerial exposure of the sediment produces thin subaerial exposure caps (vadose diagenetic caps; see Goldhammer and others, 1987). To simulate the Latemar cycles, it proved necessary to use sedimentation rates in the range of 0.10 to 0.25 m/1,000 yr. On the basis of the average ratio of exposure to submergence in these simulations, net accumulation rates are in the range of 0.05–0.125 m/1,000 yr, similar to that of the subtidal lagoons of the Bahamas (Hardie and Shinn, 1986, p. 64–65). These rates are considerably below Schlager's average "growth potential" of 1 m/1,000 yr for Holocene buildups based on margin-reef and ooid-shoal growth rates (Schlager, 1981), but they appear to be typical of the long-term accumulation rates of most ancient carbonate buildups (Schlager, 1981, Table 2). With high accumulation rates, very shallow water conditions are constantly maintained, so that the stratigraphic response to composite eustasy differs from that of the Latemar. Therefore, the discussions below, and the conclusions drawn from them, will apply only to "Latemar-type" buildups that experienced low accumulation rates.

An important aspect of these computer simulations is that the model incorporates a lag depth, which sets the minimum water depth for renewed carbonate sedimentation after subaerial exposure. Lag depth (R. N. Ginsburg, 1971, personal commun.; Hardie and Shinn, 1986) refers to the critical depth of water at which circulation becomes effective enough on the platform for carbonate production, sediment accumulation, and sediment dispersal to begin. Lag depth is estimated to be about 1–2 m, based on the characteristics of the Holocene shallowing-upward cycle that contains a basal 0.5-m-thick record of mangrove peat that overlies the Pleistocene 125,000-yr highstand surface in Florida Bay (Enos and Perkins, 1979) and the Bahamas (Harris, 1979). The peat records initial platform flooding without carbonate sedimentation because of conditions unfavorable for carbonate production. The peat is overlain by subtidal carbonate sediments, indicating that with continued rise, effective carbonate production occurred. In the Triassic Latemar carbonates, hardgrounds with oncoid lag gravels in the upper part of the subtidal member of many of the fifth-order cycles indicate that sedimentation shut down during the submergence phase of the cycle-generating sea-level oscillation (Goldhammer, 1987). Thus, a lag depth that terminates subtidal sedimentation (prior to subaerial exposure) was added to the fall portion of the high-frequency sea-level oscillation. Lag depth on the rise portion of the curve was set equal to that occurring on the fall, and both were kept constant during each run.

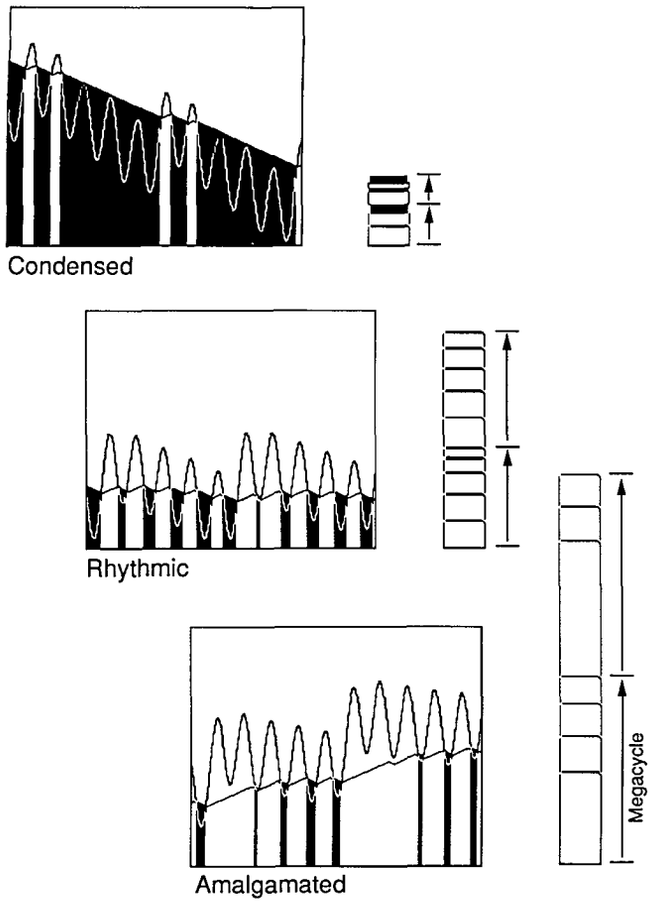

Figure 5. Graphical representation of high-frequency, composite sea-level oscillations (superimposed 100,000-yr asymmetric fourth order and 20,000-yr sinusoidal fifth order) and platform aggradation (panels on left) and resulting megacycle packaging (columns on right). High-frequency composite eustasy combined with long-term (third order) trends yields three classes of megacycles: (1) condensed megacycles are produced when one or more 20,000-yr oscillations are missed below the platform top; (2) rhythmic megacycles are produced when each successive 20,000-yr oscillation is registered; (3) amalgamated megacycles are produced when 20,000-yr oscillations are missed above the platform.

To produce a basic five-part thinning-upward megacycle of the fourth order (~100,000 yr duration) that simulates the Latemar rhythmic sedimentation, the combination of parameters must be such that the top of the platform is alternately submerged (white regions below sinusoidal sea-level curves in Fig. 5) and subaerially exposed (black areas below curves in Fig. 5) with every fifth-order (~20,000 yr duration) oscillation of sea level (Fig. 5, middle panel). Such complete five-part megacycles are referred to herein as "rhythmic megacycles" (Fig. 5, middle column; black bars are subaerial exposure caps, white is subtidal sediment); however, they might more appropriately be called "Goldilocks" megacycles because they form only when everything is just right for every fifth-order sea-level "beat" to be "caught" (that is, registered in the sedimentary record as a cycle of subtidal deposition to subaerial exposure) with metronomic regularity.

In our computer experiments, it was not difficult to induce changes in the structure of the basic thinning-upward megacycles. Relatively minor perturbations in input parameters were found to cause sea-level "beats" to be "missed" (that is, not to be registered in the sedimentary record as a cycle of subtidal deposition to subaerial exposure; see Hardie and others, 1986, p. 454). Random distributions of caught and missed beats could be caused by random variations in a host of parameters, some of which, such as erosion, were not explicitly considered in our computer modeling. The effects of random variations were not explored, but it should be possible to design appropriate experiments using stochastic models to feed in probabilistic variations in the amplitudes of successive sea-level oscillations, in sedimentation rates, and so on. We have concentrated, instead, on those conditions that favor a more systematic distribution of "missed beats." Along these lines, predictable changes in the structure of the fourth-order megacycles were found to result whenever mean sea level and its envelope of fifth-order oscillations were raised above or lowered beneath the optimum range for development of a complete rhythmic megacycle (Fig. 5). Too much water, due to a relative increase in mean sea level without a corresponding change in amplitude of the fifth-order sea-level component, would lead to prolonged submergence of the platform as sea level failed to drop below the platform top for one or more fifth-order oscillations (Fig. 5, lower panel). These "missed beats" result in incomplete megacycles (less than five cycles per megacycle) with two or more subtidal cycles amalgamated to make a much thicker than average composite cycle (Fig. 5). Because of the asymmetric "saw-tooth" shape of the fourth-order sea-level oscillations, it is the first two or three fifth-order cycles of each megacycle that become welded together into a thickened basal subtidal unit (Fig. 5, lower panel). Such incomplete megacycles are referred to herein as "amalgamated megacycles." In contrast, too little water, due to a relative decrease in mean sea level without corresponding change in amplitude of the fifth-order sea-level component, would result in periods of prolonged emergence of the top of the platform as sea level oscillated below platform level for one or more fifth-order beats (Fig. 5, upper panel). These "missed beats" produce incomplete megacycles in which the subtidal components of the registered oscillations are thinner than normal and in which the prolonged periods of emergence are recorded as unusually thick soil or tepee caps (Fig. 5). Under these low mean sea-level conditions, the "saw-tooth" shape of the fourth-order sea-level curve will keep sea level below the platform top for one or more of the last of the fifth-order beats of each fourth-order oscillation. These missed beats are nondepositional beats recorded as thickened soil or tepee caps that appear stratigraphically at the top of each megacycle (Fig. 5). This kind of incomplete megacycle is referred to herein as a "condensed megacycle." On the basis of our computer experiments, there are three sets of conditions that would favor the development of incomplete megacycles even though sea level was oscillating rhythmically in the 10^4- to 10^5-yr range.

(1) During major ice ages, the 10^5-yr asymmetric wave would dominate over the 10^4-yr sinusoidal wave (for example, Fig. 3), owing most likely to the dynamics of the melting-freezing of large ice caps. This would lead to incomplete megacycles composed of thick amalgamated subtidal units with thick soil caps, as are characteristic of Pleistocene carbonate platforms (see Perkins, 1977; Goldhammer and others, 1987).

(2) Superposition of composite fifth/fourth-order ($10^4/10^5$ yr) sea-level oscillations on a third-order (10^6 yr) sea-level rise-fall cycle can produce a systematic succession of amalgamated to rhythmic to condensed megacycle facies and systematic changes in cycle stacking patterns, as is clearly demonstrated by computer simulation (see later). This succession allows a genetic connection to be made between cyclic stratigraphy, facies stratigraphy, and sequence stratigraphy (as discussed below).

(3) Interaction of irregular pulses of subsidence (for example, stick-slip tectonic down drop) with composite high-frequency sea-level oscillations can result in a highly nonrhythmic succession of megacycles characterized by subtidal units that range from very thin (centimeters) to very thick (many meters to decameters).

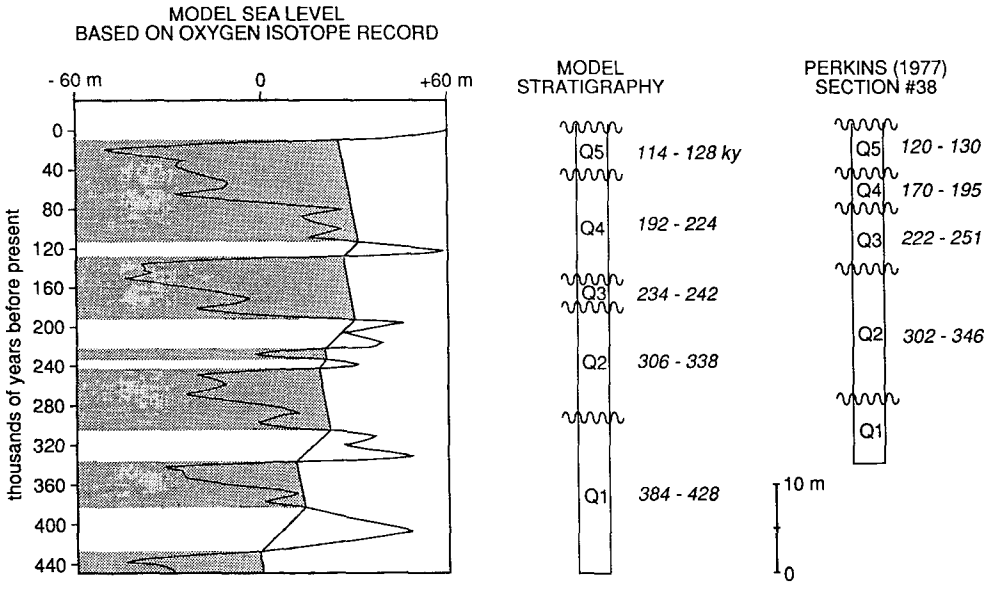

Figure 6. Computer simulation of the south Florida Pleistocene platform carbonate stratigraphy described by Perkins (1977, section 38). The Pleistocene record consists of five marine subtidal units (Q1–Q5) capped by subaerial exposure surfaces. Ages of Pleistocene units (in thousands of years) are given to the right of stratigraphic columns. Combined subsidence–sedimentation–sea-level history shown to the left. Input parameters utilized are as follows: run length = 440,000 yr; subsidence rate = 0.06 m/1,000 yr; sedimentation rate = 0.40 m/1,000 yr (see Goldhammer and others, 1987). Temporal variations in oxygen isotope data in Quaternary deep-sea sediments were used as a proxy for sea level scaled to 120-m amplitude based on Pleistocene coral reef data.

Because each of these sets of conditions produces a distinctly different stacking of megacycles, it may be possible to use these predicted differences to diagnose the underlying mechanism of cycle accumulation and to identify third-order sequences, their boundaries, and their component systems tracts (Vail, 1987) on the platform. Reported below are our efforts to apply this approach to Alpine Triassic carbonates that record unequivocal evidence of repeated episodes of submergence and subaerial exposure (Hardie and others, 1986; Goldhammer and others, 1987). Before turning to the Triassic carbonates, however, we give a brief analysis of the late Pleistocene platform carbonate cycles of south Florida. The deposition and diagenesis of these Pleistocene cycles are demonstrably related to glacio-eustatic sea-level oscillations in tune to Milankovitch rhythms, but with the amplitude of the 100,000-yr component greater than that of the 20,0000-yr component (Fig. 3). This Pleistocene system acts as an established point of reference by which to judge both the approach used in this study and the results of our analysis of the Alpine Triassic carbonates.

PLEISTOCENE OF FLORIDA: MISSED BEATS RELATED TO HIGH-AMPLITUDE FOURTH-ORDER SEA-LEVEL CHANGES

Perkins (1977) has identified five marine subtidal units (Q1 to Q5) separated by distinctive disconformities in the Pleistocene carbonates of south Florida (Fig. 6). The disconformities record periods of vadose diagenesis related to platform emergence, as evidenced by (1) laminated caliche crusts, (2) red soils and soil breccias, (3) land-plant roots, (4) karstic dissolution pipes and cavities, (5) bored surfaces, (6) fresh-water limestones, and so on (Perkins, 1977). The disconformity that separates the Holocene carbonates from the latest Pleistocene unit Q5 is well displayed in the Florida Keys, where the coral reef facies (Key Largo Limestone; Stanley, 1966) and associated subtidal grainstone-packstone facies of the upper Miami Limestone are capped by karstic cavities lined with laminated caliche crusts (Multer and Hoffmeister, 1968) and filled with red soil and coated grain breccias (Perkins, 1977). Radiometric dating of corals from this Q5 unit gives ages in the range 120,000 to 130,000 yr (Osmond and others, 1965; Broecker and Thurber, 1965). The radiometric ages of the older Pleistocene units are uncertain owing to internal inconsistencies apparently related to diagenetic alteration (Perkins, 1977), but Mitterer (1975), using amino acids in bivalve shells, has assigned ages of 170,000–195,000 yr, 222,000–251,000 yr, and 302,000–346,000 yr to units equivalent to Q4, Q3, and Q2, respectively (Fig. 6). Perkins (1977) has interpreted these Pleistocene disconformity-bounded units as the result of alternating shallow-marine deposition and subaerial exposure controlled by the Pleistocene glacio-eustatic sea-level oscillations. In a valuable discussion, Perkins (1977) has explained the distribution of facies, the position of soils, and the variations in the extent of subaerial diagenesis within a single Pleistocene unit as the effects of a sea-level rise-fall cycle operating on a seaward-sloping platform (see his Fig. 38).

In an effort to further understand the cyclicity of the south Florida Pleistocene carbonates, we attempted to simulate the Q1 to Q5 vertical succession using our "Mr. Sediment" computer program. We used the temporal variations in oxygen isotope concentrations in Quaternary deep-sea sediments (the smoothed data of Imbrie, 1985, Fig. 17) as a proxy for glacio-eustatic sea-level changes over the past 400,000 yr. We also used a sea-level amplitude scale based on Pleistocene coral reef data (Fig. 3) and then adjusted sedimentation and subsidence rates to reach as close a quantitive replica of the Q1–Q5 vertical succession as was possible (for example, as at location 38 of Perkins, 1977, Plates 2 and 3). Our simulated cyclic stratigraphy is compared with the Pleistocene succession in Figure 6. What the simulation reveals is a basic theme of "missed beats." Despite the rhythmic oscillation of sea level in tune to composite Milankovitch astronomical cycles (sinusoidal ~20,000-yr precessional beats superimposed on asymmetrical ~100,000-yr eccentricity beats, Fig. 3), only a fraction of the basic ~20,000-yr oscillations are recorded. The large amplitude of the steeply asymmetrical ~100,000-yr component carried Pleistocene sea level high enough above the top of the south Florida platform to submerge it for one or more of the initial ~20,000-yr precessional beats of each ~100,000-yr eccentricity cycle (Fig. 6). In turn, during the ~100,000-yr low stands, sea level dropped far enough below the platform top to keep it exposed for two or more of the last ~20,000-yr beats of each ~100,000-yr cycle (Fig. 6). Therefore, instead of complete 5:1 thinning-upward megacycles expected from the saw-tooth composite rhythms of the Pleistocene sea-level oscillations (as in Fig. 3), the stratigraphic record is one of incomplete megacycles with single or amalgamated subtidal units capped by extensive soils. Although it is clear from the computer simulation that the basic ~20,000-yr precessional rhythm of sea-level rises and falls has been missed, the stratigraphic succession of single and amalgamated subtidal units with their karstic soil caps has caught, with reasonable clarity, the

higher-order ~100,000-yr eccentricity rhythm (Fig. 6). In essence, the Q1, Q2, Q3-Q4 (combined), Q5, and the Holocene disconformity-bounded units are the stratigraphic records of the high stands of the ~100,000-yr component of the composite Pleistocene sea-level changes. However, the actual durations of the periods of subtidal deposition and the intervening periods of subaerial exposure are quite irregular (Fig. 6), and without the aid of accurate age dating of each cycle, it would not be possible from the cycle thickness patterns to unequivocally demonstrate that the cyclicity was controlled by externally driven rhythmic processes. Average cycle duration of this south Florida Pleistocene cyclic succession is ~67,000 yr (6 cycles in 400,000 yr), a value that does not reflect any of the actual Milankovitchian components that have shaped the Pleistocene sea-level history. The upper Pliocene to Holocene platform carbonates of the Great Bahama Bank (Beach and Ginsburg, 1978) record 15 subtidal cycles with soil caps (average thickness ~2.7 m/cycle) in the past 3.2 m.y., giving an average cycle duration of 213,000 yr. In the Bahamas, therefore, the discrepancy between the stratigraphic record of cycles and the actual rhythms of sea level that controlled accumulation is even larger than in the late Pleistocene of Florida. These anomalies are an obvious but important consequence of the phenomenon of "missed beats." Such "missed beats" may well turn out to be common in shallow-water cyclic deposits, and thus their existence may pose the largest obstacle to progress in unraveling the origins of ancient high-frequency sedimentary cycles in platform or shallow-shelf facies. It follows that identification of "missed beats" is an essential first step in any analysis of cyclic shallow-water strata. In the present study, we approached the problem by using, as end-member models, the highly rhythmic record of Ladinian cycles of the Latemar buildup (Figs. 1 and 2) and the known "missed beat" record of the late Pleistocene of the south Florida platform (Fig. 6).

NONRHYTHMIC CYCLIC SUCCESSIONS AND "MISSED BEATS" IN TRIASSIC CARBONATES OF THE ALPS

We have chosen to compare and contrast the cyclic successions of the Anisian-Ladinian of the Latemar buildup (Dolomites, Italy), the Norian Dolomia Principale (Dolomites, Italy), and the Norian Dachstein Kalk (Lofer facies) of the Northern Limestone Alps (Austria), because they appear to present a spectrum of circumstances involving "missed beats" resulting from the interaction of high-frequency sea-level oscillations (10^4–10^5 yr) with major third-order sea-level changes (10^6 yr) and tectonic movement.

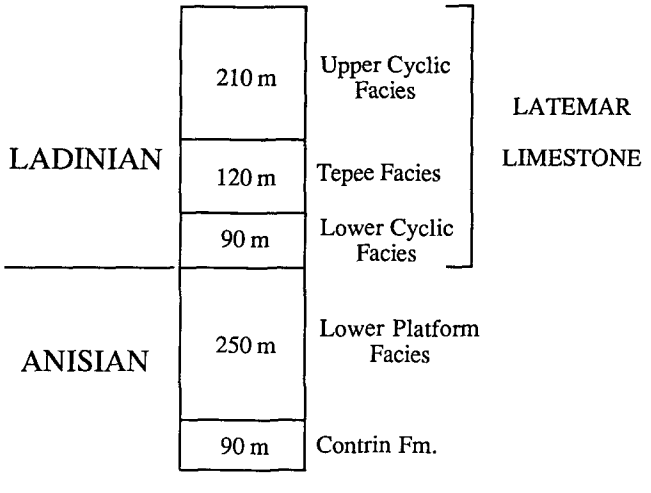

Figure 7. Stratigraphic column of facies that constitute the Latemar platform.

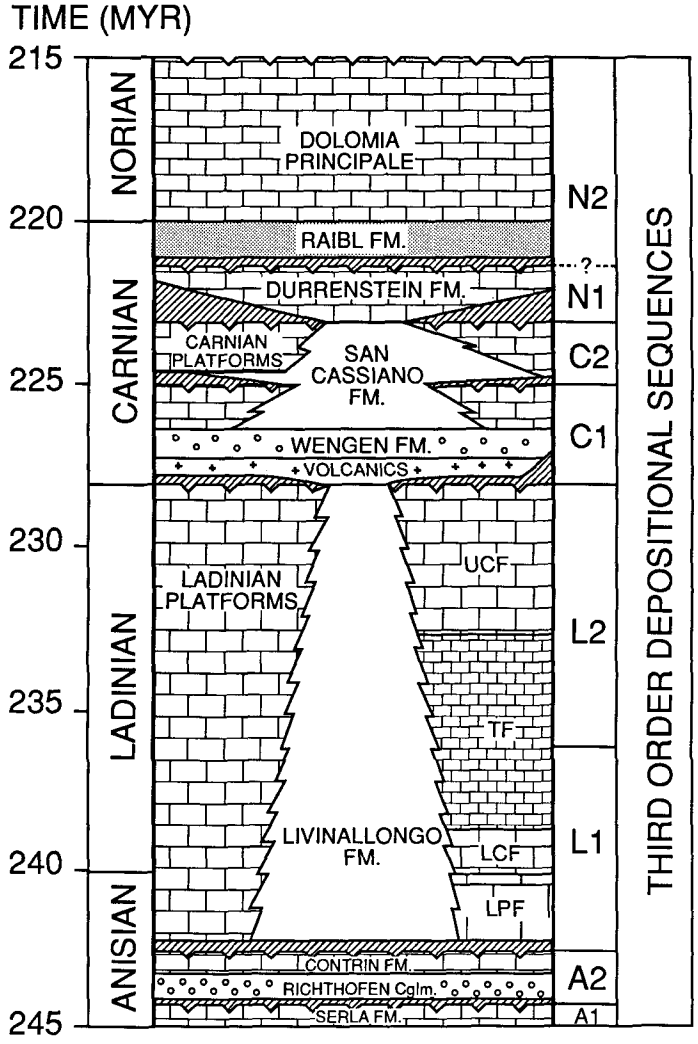

Figure 8. Middle Triassic chronostratigraphy of the Dolomites. Third-order (1- to 10-m.y. period) unconformity-bounded depositional sequences. Note that the Latemar buildup consists of two third-order depositional sequences (L1, L2). The first Ladinian sequence (L1) of the Latemar contains three stacked facies: lower platform facies (LPF), lower cyclic facies (LCF), bottom half of the tepee facies (TF). The second Ladinian sequence of the Latemar, which is incomplete, consists of the upper half of the tepee facies and the upper cyclic facies (UCF). Age dates compiled from Odin and Letolle (1982), Harland and others (1982), and Haq and others (1987). The duration of the Ladinian sequences was constrained by counting the number of fifth-order cycles in the Latemar buildup (see text).

Anisian-Ladinian of the Latemar Buildup

A Systematic Succession of Megacycles Related to a Complete Third-Order Sea-Level Oscillation. The Latemar buildup (800 m thick; 5–6 km wide) of late Anisian–Ladinian age is one of several well-exposed Middle Triassic carbonate platforms in the Dolomites of northern Italy (Bosellini and Rossi, 1974; Bosellini, 1984). The flat-lying platform succession of the Latemar records three superimposed orders of stratigraphic cyclicity, including (1) a long-term, third-order depositional sequence (460 m thick; approximately 8 m.y. duration, sequence L1); (2) fourth-order megacycles (subdecameter scale; approximately 100,000 yr duration);

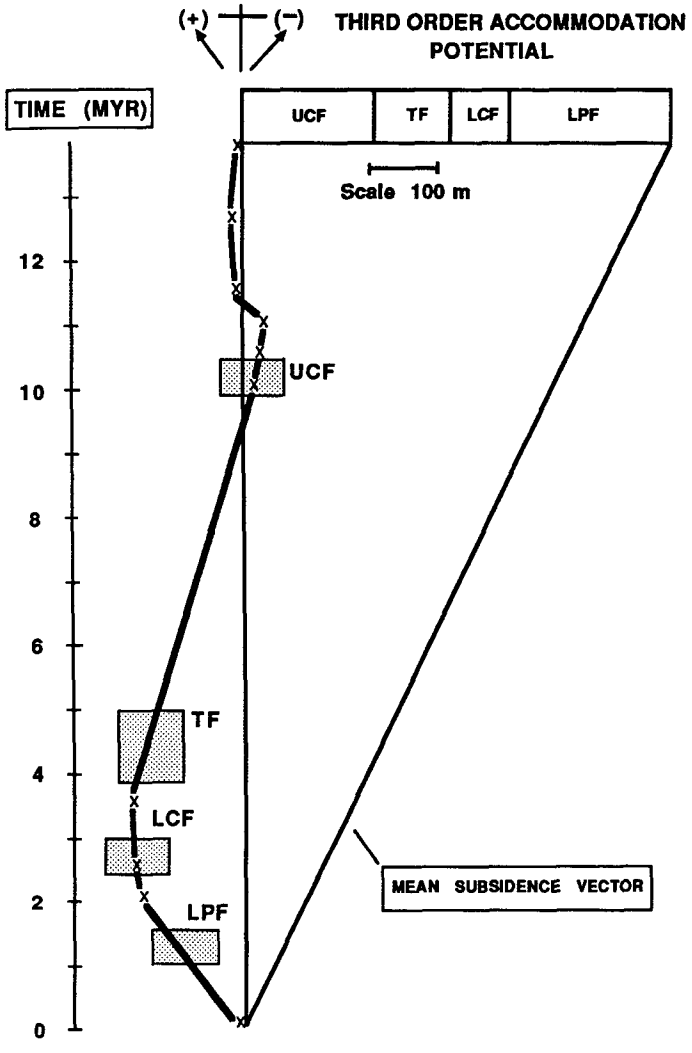

Figure 9. Third-order accommodation potential determined by long-term "Fischer plot" (Fischer, 1964; Goldhammer and others, 1987; Goldhammer, 1987) of the entire Latemar platform succession (only the long-term trace of the approximately 500 individual fifth-order cycles is shown). Vertical axis depicts the total amount of geologic time (in millions of years), and the duration of each facies was derived by counting fifth-order cycles, assuming 20,000 yr/cycle. Mean subsidence vector represents constant background subsidence of the platform and represents average rate of sediment accumulation. Deviations (plus or minus) from the mean subsidence rate are interpreted as third-order eustatic sea-level changes after correction for isostatic loading. Representative time-stratigraphic intervals used in comparing actual stratigraphy and computer-simulated stratigraphy of each facies (for example, Figs. 10–13) are shown as shaded boxes (LPF, lower platform facies; LCF, lower cyclic facies; TF, tepee facies; UCF, upper cyclic facies). The simulated stratigraphy of these intervals is generated by superimposing three different orders of eustasy—high-frequency fourth (~100,000 yr) and fifth (~20,000 yr) atop long-term third (~10 m.y.)—under conditions of constant sedimentation and linear background subsidence. The shape, period, and amplitude of third-order change is taken directly from the long-term "Fischer plot," and background subsidence is taken as the mean subsidence vector.

(3) fifth-order cycles (submeter to meter scale; approximately 20,000 yr duration).

The Latemar platform contains four vertically stacked, aggradational facies (Fig. 7 and sequences L1, L2 in Fig. 8): (1) lower platform facies (LPF), 250 m of subtidal, shelf-lagoon carbonate punctuated by thin subaerial exposure horizons roughly every 10 m on average; repetitive meter-scale, fifth-order cycles are lacking; (2) lower cyclic facies (LCF), 90 m of fifth-order, meter-scale cycles (73 cycles; average 1.24 m/cycle), each composed of bioturbated, subtidal shelf-lagoon carbonate overlain by a thin (5–15 cm thick) vadose, dolomitic caliche crust; fifth-order cycles are grouped into asymmetric, thinning-upward megacycles; (3) tepee facies (TF), 120 m of meter-scale, fifth-order cycles (295 cycles; average 0.4 m/cycle), periodically interrupted by tepee zones recording extended subaerial exposure; fifth-order cycles are grouped into thinning-upward megacycles capped by tepees; (4) upper cyclic facies (UCF), 210 m of fifth-order cycles (230 cycles; average 0.96 m/cycle) similar to the lower cyclic facies.

The vertical facies succession of the lower platform facies to lower cyclic facies to lower half of the tepee facies defines a third-order depositional sequence (sequence L1, Fig. 8) generated by a long-term third-order relative rise-fall sea-level cycle. The basal sequence-bounding unconformity occurs at the top of the middle Anisian Contrin Formation, and the sequence is capped by a transitional boundary marked by a complex 13-m-thick tepee interval (Goldhammer and Harris, 1989). The upper half of the tepee facies and the overlying upper cyclic facies represent the beginning of another sequence (sequence L2, Fig. 8).

The first Latemar sequence records systematic changes in stratigraphic and lithologic character that reflect progressively decreasing third-order accommodation potential, that is, the sum of long-term third-order eustatic sea-level changes plus background platform subsidence. First of all, the lower platform facies differs from the other facies in that it lacks repetitive meter-scale fifth-order cycles. Instead, subtidal deposits are punctuated by subaerial exposure caps on average approximately every 10 m (nonrhythmically, as confirmed by autocorrelation tests). In contrast, within the overlying facies (lower cyclic and tepee facies), fifth-order cycles (as described and discussed by Goldhammer and others, 1987) occur with regularity and decrease in thickness overall from the base of the lower cyclic facies (individual cycles as much as 4 m thick) to the middle of the tepee facies (individual cycles <0.5 m thick). This progression from a noncyclic interval to cyclic intervals marked by decreasing cycle thickness upward indicates that third-order accommodation potential (that is, accumulation space available for fifth-order cycle aggradation) for each depositional pulse was reduced. Secondly, the proportion of marine submergence (and concomitant early marine diagenesis) to subaerial exposure (and concomitant subaerial diagenesis) varies systematically upward through the sequence. The lower platform facies is dominated by subtidal deposits full of early marine syndepositional diagenetic features (hardgrounds, sheetcracks, early marine cements; Goldhammer, 1987). In contrast, evidence for such intensive early marine diagenesis is lacking in the overlying lower cyclic and tepee facies, which contain vadose diagenetic features (caliche fabrics, vadose cements; Goldhammer and others, 1987; Goldhammer, 1987). The progressive increase in subaerial-exposure features clearly records a shift from generally submergent conditions during lower platform facies deposition to conditions whereby subtidal deposition was frequently interrupted by intervals of subaerial exposure (lower cyclic and tepee facies). Thus, the stratigraphic variation of early diagenesis parallels the changes in cycle thickness as both respond to decreasing third-order accommodation potential.

In a qualitative sense, then, the vertical facies stacking and cycle stacking patterns clearly record a third-order relative sea-level change. The

question remains, can this third-order variation be treated quantitatively to extract information regarding rates, periodicity, and amplitude of third-order change? By utilizing fifth-order cycles as stratigraphic time units equal to 20,000 yr, a third-order accommodation-potential curve can be constructed via graphical time-space analysis of the entire Latemar platform succession (Fig. 9). This method, originally outlined by Fischer (1964), graphically portrays long-term deviations from mean subsidence (assumed constant, or at least changing at a very slow rate over the time span of the Latemar buildup). Such deviations are generated by the cumulative effect of progressive changes in fifth-order cycle thicknesses, which are plotted successively against time, assuming each cycle is of 20,000 yr duration (see Fischer, 1964, p. 146–148, and Goldhammer and others, 1987, p. 869–874, for discussion of graphical time-space analysis). This Fischer diagram (Fig. 9) contains only the trace of the long-term change (individual fifth-order cycles, which plot as discrete triangles, are not shown; compare, for example, with Fig. 2) and illustrates deviations from mean subsidence (approximately 5 cm/1,000 yr) plotted against the Latemar stratigraphy. Positive deviations (shifts to the left) depict increased relative third-order rise in sea level or increase in accommodation. Negative deviations (shifts to the right) mark relative third-order fall or decrease in accommodation. The curve, which forms an asymmetric cycle of positive (thick accumulation) to negative (thin accumulation) deviations, substantiates the notion that the first Latemar third-order sequence (lower platform facies to lower cyclic facies to lower half of the tepee facies) represents progressively decreasing third-order accommodation potential. Inherent error in the analysis stems from the "missed beats" of fifth-order eustasy recorded in the lower platform and tepee facies; thus, the time derived for each facies and the entire Latemar platform succession is a minimum. Within the tepee facies, fourth-order megacycles with tepee caps were assigned 100,000-yr durations, even if fewer than 5 fifth-order cycles were present. For the lower platform facies, the duration was constrained by age dates and computer simulations of the entire Latemar buildup (Goldhammer, 1987). The third-order trend (Fig. 9), which forms a cycle of relative rise and fall, is interpreted as a eustatic sea-level change with an amplitude of approximately 60 m (after correction for isostatic loading) and a period of about 8 m.y. (Goldhammer, 1987).

The Significance of the Cyclic Facies: Rhythmic Megacycles. As discussed above, the cyclostratigraphy of the cyclic facies of the Latemar buildup provides the basic evidence for rhythmic sedimentation during the Triassic. The stacking patterns of the five-part thinning-upward megacycles of these facies indicate a rhythmic depositional response to a composite high-frequency (fourth and fifth order) eustasy in the Milankovitch band. These Latemar rhythmic megacycles are our "Goldilocks" megacycles that appear to have recorded almost every single fifth-order (approximately 20,000 yr) sea-level oscillation. Such a complete record of high-frequency composite eustasy was found to be most precisely simu-

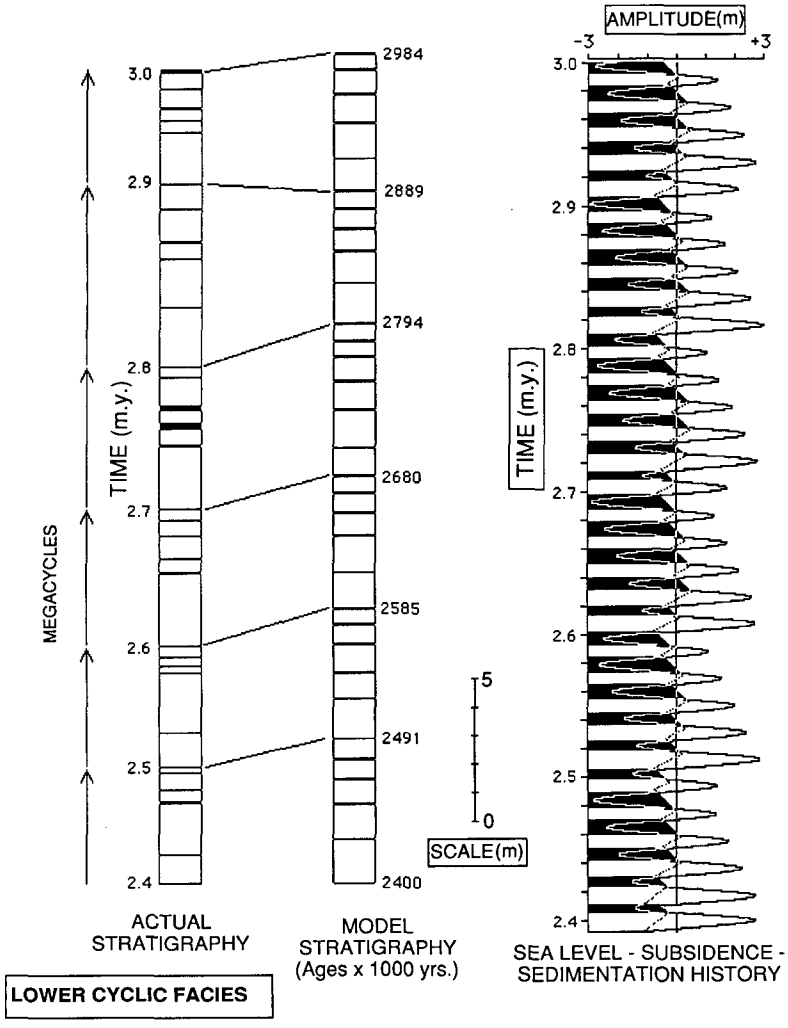

Figure 10. Direct comparison of the actual stratigraphy of the lower cyclic facies and computer-generated stratigraphy for a 600,000-yr time interval of the Latemar buildup. Thicker white layers in the stratigraphic columns (left) mark subtidal parts of cycles; thin black layers mark subaerial exposure caps. The simulated interval is between 2.4 and 3.0 m.y. of the total 12 m.y. of geologic time that the buildup records. Actual and simulated fourth-order megacycles are correlated on the basis of actual versus modeled age dates. The sea-level–subsidence–sedimentation record to the right of the stratigraphic column represents the shaded box labeled LCF in Figure 9. The amplitude of ±3 m refers only to high-frequency (fourth and fifth order) eustasy. Model variables used in this and the simulations shown in Figures 11, 12, and 13 are (a) fifth-order eustasy—sinusoidal shape, 2-m amplitude, 19,000-yr period; fourth-order eustasy—asymmetric shape (sawtooth), 1-m amplitude, 103,000-yr period; third-order eustasy—shape, amplitude (60 m), and period (~10 m.y.) taken directly from the long-term "Fischer plot" (Fig. 9); (b) linear subsidence—0.05 m/1,000 yr (equal to the mean subsidence vector of the long-term "Fischer plot," (Fig. 9); (c) uniform sedimentation rate—0.15 m/1,000 yr; (d) lag depth—1 m (on fifth-order rise and fall); (e) rate of soil cap development—0.01 m/1,000 yr.

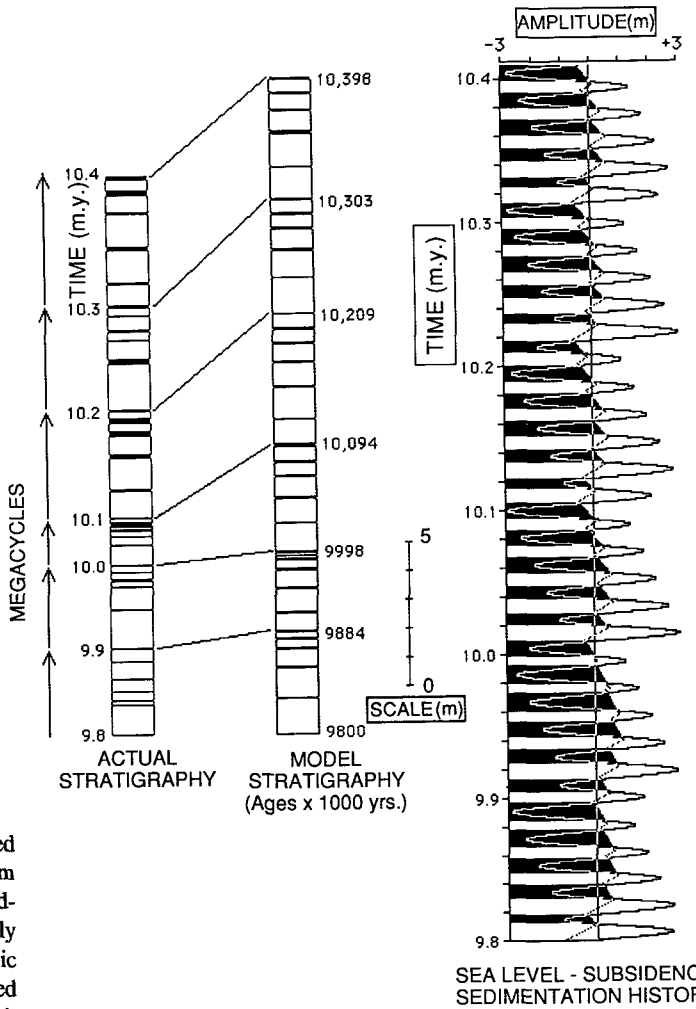

Figure 11. Direct comparison of the actual stratigraphy of the upper cyclic facies and computer-generated stratigraphy for a 600,000-yr time interval of the Latemar buildup (interval between 9.8 and 10.4 m.y., shaded box labeled UCF in Fig. 9). See text and Figure 10 for run input data.

UPPER CYCLIC FACIES

lated by computer under conditions wherein the effect of superimposed third-order sea-level changes was minimal (for example, Fig. 4). Optimum conditions should occur at the crests and troughs of such long-term third-order waves when the rate of third-order eustatic change is theoretically zero. As can be seen in Figure 9, these are precisely where the lower cyclic (third-order crest) and upper cyclic (third-order trough) facies are located in the Latemar third-order succession. Figures 10 and 11 show comparisons between actual stratigraphies of the lower and upper cyclic facies of the Latemar and simulated stratigraphies generated by "Mr. Sediment." The model stratigraphies shown in Figures 10 and 11 were generated by superimposing short-term composite eustasy (combined fourth- and fifth-order effects) on top of long-term changing accommodation potential (combined third-order eustasy plus background platform subsidence) derived from the Fischer diagram of the Latemar buildup (Fig. 9). The simulations yield complete five-part rhythmic megacycles without any missed depositional beats of fifth-order eustasy, and thus, the stratigraphic record is complete. Additionally, note the roughly equivalent proportion of submergence time to subaerial-exposure time for individual cycles and megacycles (white striped versus black striped areas on the model sea-level–subsidence– sedimentation record).

The Significance of the Lower Platform Facies: Amalgamated Megacycles. On the basis of analysis of the Latemar cyclic facies, we conclude that Milankovitch-driven glacio-eustatic sea-level oscillations were operating throughout the entire accumulation of the buildup and were dictating the development of fifth-order cycles and their arrangement into fourth-order megacycles. We must then consider the significance of those facies that do not contain an uninterrupted succession of meter-scale cycles grouped into megacycles.

The lower platform facies is characterized by subtidal skeletal-lithoclastic packstone-grainstone containing overwhelming evidence for abundant early marine diagenesis (submarine cemented sheetcracks, submarine hardgrounds, a variety of early marine cement types, and so on; Goldhammer, 1987). Subaerial exposure surfaces, similar to those in the overlying cyclic facies, are relatively uncommon, occurring every 10 m or so on average. The lower platform facies is interpreted as primarly subtidal in origin (shallow, back-margin lagoon), and depositional conditions were marked by subtidal sedimentation and submarine diagenesis. Submarine sedimentary hiatuses and syndepositional marine diagenesis are very common, whereas subaerial depositional breaks are not, pointing at generally submergent conditions and a predominantly subtidal origin.

The lower platform facies lacks repetitive meter-scale cycles arranged in five-part megacycles (Fig. 12). Relative time-series analysis and graphical time-space analysis failed to identify any rhythms (Goldhammer, 1987). Instead, the lower platform facies consists of thick "cycles" of subtidal carbonate punctuated by thin subaerial exposure caps approximately one every 10 m. By comparison with the average fifth-order cycle thickness for the Latemar cyclic facies (average <1 m/cycle), these lower platform facies "cycles" are too thick and occur too infrequently to be considered fifth-order cycles of 20,000 yr duration. Rather, each "cycle" must represent the amalgamated record of several fifth-order sea-level beats that oscillated above the platform top and so failed to expose the platform. On the basis of the lower platform facies thickness and age constraints, third-order accommodation potential was greatest during lower platform facies accumulation (Fig. 9).

Computer simulations of the lower platform facies reveal how this maximum accommodation potential interacted with short-term composite

sea level and constant subtidal accumulation rates to generate the lower platform facies stratigraphy (Fig. 12). All other input variables (for example, subtidal accumulation rates, lag depth, and so on) are identical to those utilized in simulations of the Latemar cyclic facies, and only long-term accommodation potential has changed by adding in the effects of a rising third-order sea-level component. The lower platform facies simulation produces subaerial exposure surfaces approximately every 8 m on average, and thick subtidal packages are generated as a result of several "missed beats" of subaerial exposure, during which time amalgamated subtidal fifth-order cycles (without subaerial exposure caps) were produced by each asymmetric fourth-order megacycle (that is, approximately 100,000 yr). In the simulation, the approximately 20,000-yr sinusoidal rhythms oscillated above the top of the platform and in most instances failed to expose the platform. Therefore, no repetitive fifth-order, meter-scale cycles or complete fourth-order megacycles (composed of five fifth-order cycles) were formed. Rather, "incomplete" amalgamated megacycles resulted. The model sea-level–subsidence–sedimentation record (Fig. 12) also illustrates the manner in which lower platform facies sediments were subject to long, uninterrupted periods of marine submergence favoring abundant marine diagenesis. The effect of lag depth in shutting down sedimentation on the falling limb of each sinusoidal wave yields periods of nondeposition, during which time early marine diagenesis could be concentrated at a nonaggrading surface to produce hardgrounds and submarine tepees.

The lower platform facies stratigraphy interpreted in light of "missed beats" is a good illustration of Sander's Rule. Despite rhythmic periodicity of the cycle-producing mechanism (for example, Milankovitchian glacio-eustasy), the corresponding stratigraphic record may not preserve every cycle-producing pulse as a stratigraphic cycle. The record is thus incomplete, as fifth-order cycles are hidden in an amalgamated subtidal record.

The Significance of the Tepee Facies: Condensed Megacycles. Separating the rhythmic megacycle successions of the lower and upper

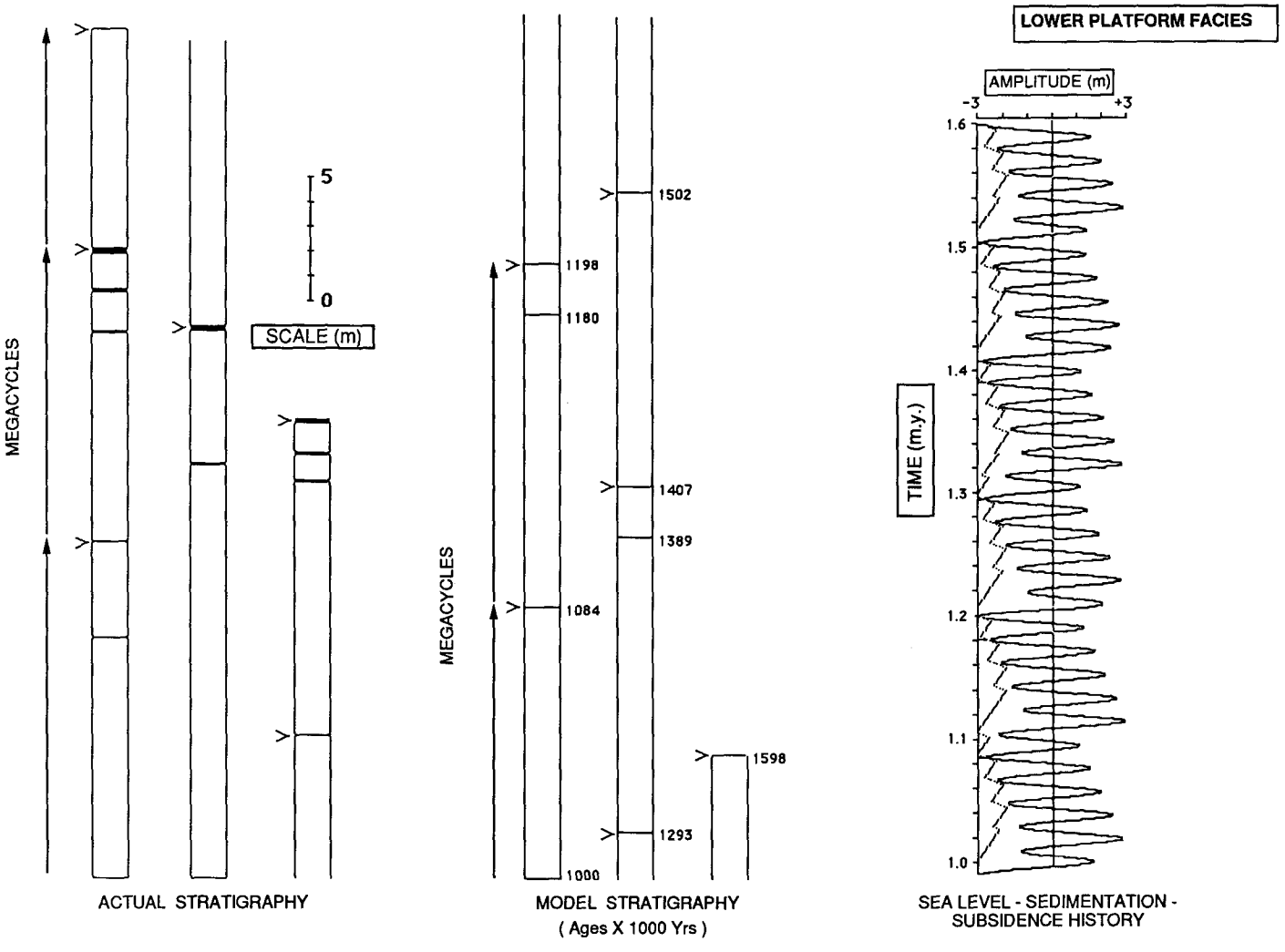

Figure 12. Direct comparison of the actual stratigraphy of the lower platform facies and computer-generated stratigraphy for a 600,000-yr time interval of the Latemar buildup (interval between 1 and 1.6 m.y., shaded box labeled LPF in Fig. 9). Representative stratigraphic section of the lower platform facies consists of thick (2–15 m) intervals of subtidal deposits (white in the stratigraphic columns) punctuated by thin subaerial exposure caps (thin black layers). Correlation of actual and simulated megacycles is based on stacking patterns and thickness of smaller "cycles." See text and Figure 10 for run input data.

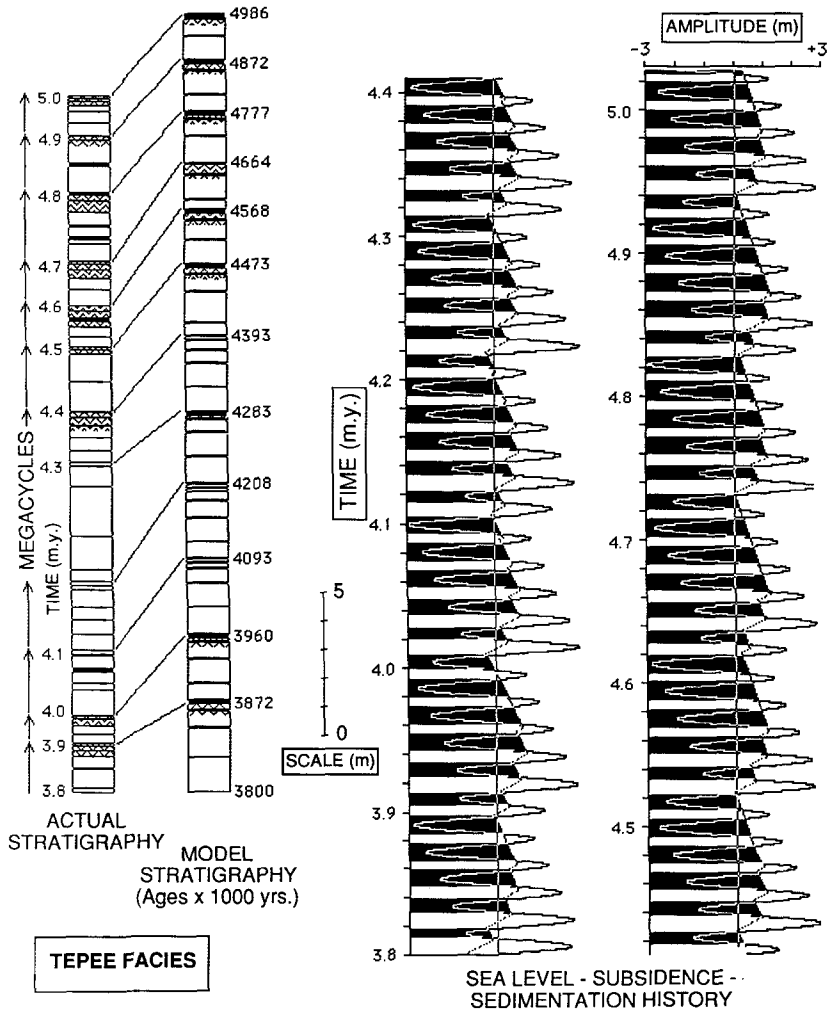

Figure 13. Direct comparison of actual stratigraphy of the tepee facies and computer-generated stratigraphy for a 1.2-m.y. time interval of the Latemar buildup (interval between 3.8 and 5.0 m.y., shaded box labeled TF in Fig. 9). Representative stratigraphic section of the tepee facies consists of interstratification of normal thinning-upward megacycles and megacycles with tepee caps. Tepees are composed of one to three disrupted fifth-order cycles (zig-zag pattern in stratigraphic column). Correlation of actual and simulated megacycles is based on stacking patterns combined with a comparison of actual and modeled age dates. See text and Figure 10 for run input data.

cyclic facies is a 120-m-thick interval characterized by 35 discrete tepee zones (Hardie and others, 1986), distributed vertically throughout the section, that add a different component to the normal cyclic pattern (Fig. 13). Tepee zones are interbedded with zones of fifth-order cycles that are analogous to those of both of the cyclic facies. Individual tepees (typically 1–2 m thick) are antiform structures that have fairly symmetrical, chevron-like cross sections, displaying flat bases with uparched tepee crests separated by inter-tepee depressions. Tepee crests are truncated by overlying beds that thin laterally as they onlap the flanks of tepee crests, indicating the syndepositional origin of the structures. The most significant aspect of Latemar tepees is that they consist of buckled and disrupted fifth-order Latemar cycles (that is, subtidal limestone with thin vadose diagenetic caps) identical to those that occur between tepees and identical to those that characterize both Latemar cyclic facies (Hardie and others, 1986). The vast majority of tepee zones occur as thin (<2 m) disrupted caps to single megacycles, but there are a few unusually thick (3–13 m) tepee zones that are highly brecciated and involve more than one megacycle. In the tepee zones that cap single megacycles, the number of cycles incorporated varies from one to four, each cycle being on the order of 0.10 to 0.40 m thick. Tepees are interpreted as the product of expansive cementation of pre-existing thin fifth-order cycles. Tepees are associated with sediments that were subaerially exposed (that is, vadose caps of cycles), and the presence of extensive vadose diagenetic features within tepees (fitted pisoids, vadose stalactitic cements, dissolution vugs; Hardie and others, 1986; Goldhammer, 1987) argues for an origin primarily related to subaerial exposure.

The presence of thinning-upward, fourth-order megacycles between tepees indicates that the same composite, eustatic sea-level rhythm responsible for both the Latemar cyclic facies operated during deposition of the tepee facies. Despite the overprint of tepee formation, an accurate counting of cycles within individual tepees is possible and reveals that the normal composite cycle rhythm can still be read, as verified by both graphical time-space and relative time-series analyses (Fig. 14; Goldhammer, 1987). Tepees composed of disrupted thin fifth-order cycles occur as tops to megacycles marked by thicker basal cycles. Fourth-order megacycles with tepee caps may contain five fifth-order cycles, but commonly they are incomplete, containing only three or four fifth-order cycles (Figs. 13 and 14). We interpret these incomplete tepee-capped megacycles as "condensed" fourth-order megacycles that do not record all depositional pulses of the composite eustatic sea-level curve. These condensed megacycles have missed one or more of the fifth-order depositional beats on the falling limb of the fourth-order wave.

On the basis of the thickness of the tepee facies and age constraints (derived by counting fifth-order cycles, assuming 20,000 yr per cycle), third-order accommodation potential was least during tepee facies accumulation (Fig. 9). Computer simulations of the tepee facies demonstrate the manner in which condensed megacycles were generated by missing one or more of the fifth-order pulses during the falling phase of the asym-

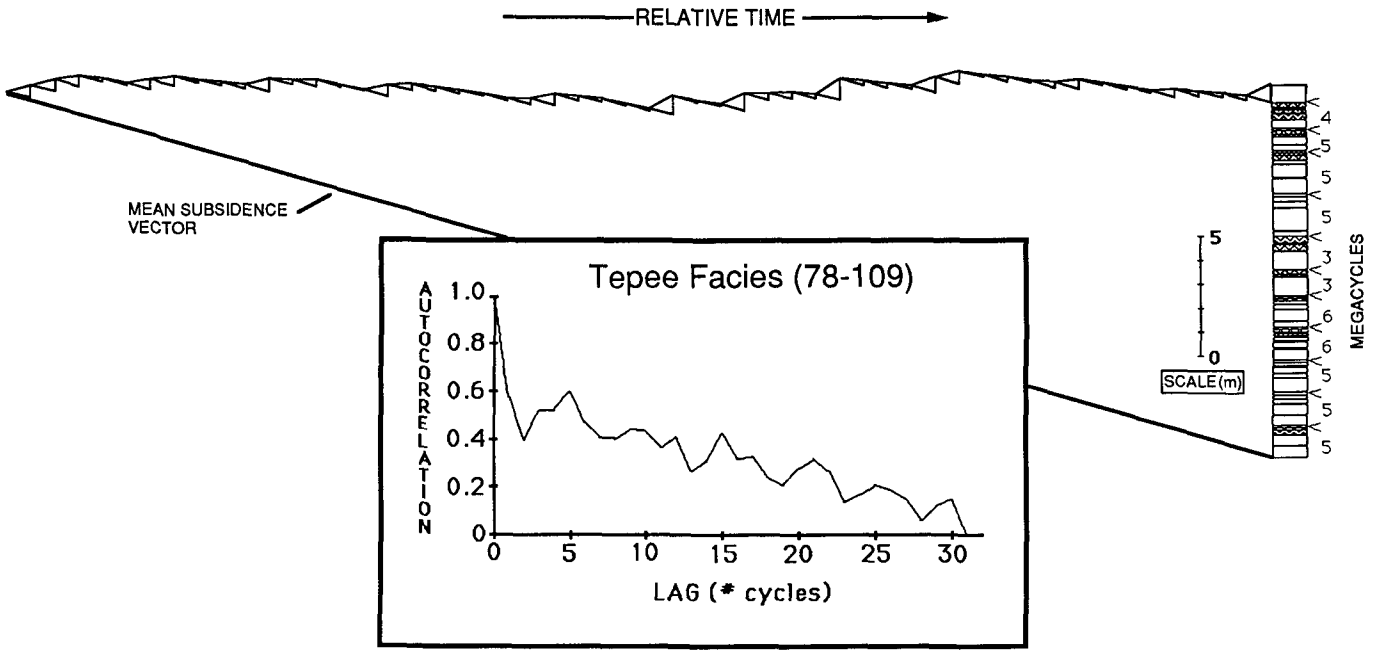

Figure 14. "Fischer plot" and time-series analysis of a portion of the stratigraphic succession of cycles in the tepee facies. Taking into account the number of fifth-order cycles incorporated into a tepee zone (cycles with zig-zag pattern) and applying these techniques reveal a cycle packaging similar to that found in the lower and upper cyclic facies (compare this figure with Fig. 2).

metric fourth-order sea-level oscillation (Fig. 13). All input variables are identical to those utilized in simulations of the cyclic facies and the lower platform facies except that long-term accommodation potential, upon which composite short-term eustasy is riding, has been changed by adding in the effects of a falling third-order sea-level component. The resulting reduced accommodation potential ensured that the lower one or two basal fifth-order cycles of a megacycle would aggrade high enough so that the subsequent fifth-order oscillations could not rise above lag depth, or in some cases, above the platform top, thus resulting in missed depositional cycles. During these missed depositional beats in the regressive portion of a megacycle, the pre-existing fifth-order cycles that formed at the front end of the fourth-order sea-level oscillation were subject to prolonged subaerial exposure and disrupted into tepees. Lag depth on the falling limb of each fifth-order sinusoidal beat had the effect of ensuring the formation of thin cycles that were most susceptible to disruption into tepees. Tepee simulation was achieved by inputting an upper limit on the thickness of the subaerial exposure cap of fifth-order cycles. During prolonged subaerial exposure, when a diagenetic cap of a fifth-order cycle achieved a thickness of 0.10 m, a routine within "Mr. Sediment" stopped diagenetic cap development and instead graphically overprinted pre-existing cycles with a zig-zag pattern at a fixed rate similar to that of the rate of soil formation to simulate the genesis of tepees. The upper limit of diagenetic cap thickness of 0.10 m was based on observations that known examples of Holocene tepees have indurated crust thicknesses that rarely exceed 10 cm (data in Goldhammer, 1987) together with the observation that diagenetic cap thicknesses of fifth-order cycles involved in Latemar tepees never exceed 10 cm.

The stratigraphy of the tepee facies, combined with the computer simulations, provides a further illustration of Sander's Rule where rhythmic, potentially cycle-producing fifth-order beats of eustasy are "missed," that is, not preserved as stratigraphic cycles. Inspection of the sea-level–subsidence–sedimentation history (Fig. 13) illustrates how such "missed beats" of cycle deposition, which occurred on the falling limb of the fourth-order oscillation, resulted in condensed megacycles with a strong vadose diagenetic overprint. Because of reduced accommodation potential imposed by third-order sea-level fall tracking subsidence, the relative proportion of submergence time to subaerial-exposure time is reduced for each megacycle as compared to the underlying lower platform facies and lower cyclic facies. Note also that the very thin cycles characteristic of the tepee facies are not the result of reduced sedimentation rates, nor of reduced cycle duration, but rather of reduced accommodation space.

Eustatic Model for the Systematic Succession of Latemar Megacycles. Long-term computer simulations quantitatively illustrate the effect of composite eustatic sea-level oscillations on both the small-scale stratigraphic variability (that is, meter-scale cycles, tepees, and so on) and the large-scale vertical stratigraphic packaging and closely simulate the actual Latemar stratigraphy (Figs. 10 through 13). Representative parts of each of the Latemar platform facies were simulated by superimposing high-frequency fourth- and fifth-order eustasy atop long-term third-order eustasy (taken directly from the graphical time-space analysis) under conditions of constant subsidence (that is, mean subsidence of 5 cm/1,000 yr) and constant subtidal accumulation rates (15 cm/1,000 yr; Goldhammer, 1987). In the representative simulations, all variables (that is, amplitudes of high-frequency eustasy, periods of fourth- and fifth-order change, lag depth, and so on) were fixed; only long-term third-order sea level was allowed to vary (Fig. 9).

On the basis of these simulations and in the spirit of Sander's Rule, a eustatic model for the development of the Latemar vertical facies stacking under conditions of constant subsidence can be formulated as follows (Fig. 9).

(1) *Lower platform facies* (Fig. 12)—Prolonged, relatively rapid, third-order sea-level rise dominates the system, maximizing third-order accommodation potential, maintaining subtidal conditions over the entire

platform. Subtidal sedimentation is unable to keep up, and thus not every beat of fifth-order, high-frequency sea level can "touch down" on the platform top and subaerially expose the top of the sediment column. These "missed beats" of subaerial exposure result in the formation of thick (average approximately 10 m), fourth-order amalgamated megacycles. During this phase of subtidal carbonate aggradation, subaerial exposure occurs infrequently, and lengthy periods of marine submergence promote abundant syndepositional marine diagenesis.

(2) *Lower cyclic facies* (Fig. 10)—During development of the lower cyclic facies, the rate of third-order rise progressively declines as the crest of the third-order wave is approached, resulting in reduced third-order accommodation potential. Now, subtidal sedimentation can keep up with net sea-level change, which near the third-order crest, is due almost entirely to subsidence. Under these conditions, every fifth-order, high-frequency oscillation can subaerially expose the top of the sediment column and form a legible cycle boundary. Thus, fully developed, fourth-order, rhythmic megacycles with roughly equivalent durations of submergence and exposure are formed. The progressive slowing of third-order rise results in sequentially thinner cycles upward from the base to the top of the lower cyclic facies.

(3) *Tepee facies* (Fig. 13)—During the evolution of the tepee facies, third-order sea level is falling and third-order accommodation potential is minimized, but in a realm of continuous subsidence, the net effect is close to but not quite that of a stillstand. Now, sedimentation easily keeps up and very thin cycles form (thinner than those of the lower cyclic facies), which are grouped into fourth-order condensed megacycles with tepee tops representing more lengthy periods of subaerial exposure. The tepees form owing to prolonged subaerial exposure during the falling limb of a fourth-order oscillation. The first Latemar third-order sequence (sequence L1, Fig. 8) is capped by a complex interval (13 m thick) of numerous thin, superimposed tepee zones in the middle of the tepee facies, which we interpret as the upper sequence boundary. With a decline in the rate of third-order fall, the rate of decreasing accommodation declines, and thicker, tepee-capped, condensed megacycles form the upper half of the tepee facies and the start of another third-order sequence.

(4) *Upper cyclic facies* (Fig. 11)—As the third-order sea-level fall that deposited the tepee facies bottomed out, the accommodation potential increased again. This resulted from a near-zero rate of change of third-order sea level in the trough of the third-order wave, so that at this stage, subsidence controlled the accumulation space. The upper cyclic facies therefore is a replica of the lower cyclic facies, formed under the same "Goldilocks" conditions that produce rhythmic megacycles but this time in the trough rather than the crest of the third-order sea-level oscillation. In keeping with our eustatic model, the upper cyclic facies succession exhibits thicker cycles and upward-thickening of rhythmic megacycles as the third-order sea level begins a new oscillation near the end of the Ladinian. The upper boundary of the upper cyclic facies has been removed by Quaternary erosion of the top of the Latemar buildup, but other coeval buildups are capped by a regionally widespread unconformity and overlain by volcanic and volcaniclastic rocks related to a late Ladinian–early Carnian volcano-tectonic event that catastrophically terminated the Anisian-Ladinian phase of carbonate buildups in the Southern Alps (Bosellini, 1984).

In summary, the first Latemar third-order sequence (that is, sequence L1; lower platform facies to lower cyclic facies to tepee facies) is characterized by a systematic succession of amalgamated to rhythmic to condensed fourth-order megacycles, which is a direct consequence of three superimposed orders of sea level. Despite the existence of temporal eustastic rhythms (that is, metronomic fourth- and fifth-order eustasy) a marked inequality exists between the thickness of the stratigraphic record and the actual time it represents. For example, the lower platform facies is 250 m thick and records about 2 m.y. of geologic time. In contrast, the tepee facies is considerably condensed, recording approximately 6 m.y. of geologic time in 120 m of section. These considerations are readily comprehended in light of Sander's Rule and composite eustasy impelled by third-order changes. It follows that in shallow-water platform deposits, facies and cycle thicknesses are not directly proportional to cycle duration but instead are a function of accumulation space. This poses obvious and serious difficulties for any time-series approaches that equate cycle thickness with cycle duration.

Norian Cyclic Platform Carbonates

The widespread blanket of Norian platform carbonates provides a style of Alpine Triassic meter-scale cyclic deposition related to composite sea-level oscillations different from that of the Ladinian just considered. The stratigraphic units represented here are the Norian Dolomia Principale in the Southern Alps (Fig. 8) and its stratigraphic equivalent, the Hauptdolomit and Dachsteinkalk, with its well-known Lofer facies, in the Northern Limestone Alps. These Norian cyclic platform carbonates, which cover a very large part of the Alpine region, represent accumulation mainly during the lengthy fall of a very asymmetrical third-order sea-level cycle that occupied the entire Norian stage of the Triassic (Haq and others, 1987). At the same time, subsidence varied considerably from locality to locality; for example, the Dolomia Principale reaches 1,500 m thick in the Belluno and Lombard basins but is only 250 m thick on the intervening Trento Plateau fault block (Hardie and others, 1986). Therefore, in addition to the overall third-order sea-level fall, local differential subsidence related to tectonics must have been an important influence on cyclic sedimentation in the Alps during the Norian.

The Norian Dolomia Principale: Systematic Changes in Condensed Megacycles Related to a Slow Third-Order Sea-Level Fall. In Norian time, the entire Southern Alps region was blanketed by the 250- to 1,500-m-thick platform carbonates of the Dolomia Principale (Bosellini, 1965, 1967). In the Dolomites region of the Southern Alps, the Dolomia Principale consists of two main facies, a cyclic peritidal facies and a subtidal facies (Fig. 15; see also Bosellini and Hardie, 1985), both of which are completely dolomitized. The cyclic peritidal facies is a stack of meter-scale, shallowing-upward cycles capped by mudcracked, cryptalgal laminites (Bosellini, 1965, 1967; Bosellini and Hardie, 1985). In contrast, the subtidal facies consists of 0.15- to 5-m-thick (average 1.5 m/cycle) "diagenetic cycles," each made of a subtidal unit with a subaerial exposure cap containing evidence for vadose diagenesis (caliche fabrics, vadose pisoids and cements, and so on; Hardie and others, 1986; Bosellini and Hardie, 1985). These subtidal cycles with subaerial exposure caps must be the result of relative sea-level oscillations, which based on the number of cycles and time intervals involved, occurred with an average frequency of 24,000 to 40,000 yr/cycle, using the radiometric age dates of Harland and others (1982) and Odin and Letolle (1982), respectively. The cycles are therefore fifth-order stratigraphic cycles.

The subtidal unit is a massive, vuggy dolomite composed primarily of peloid and grapestone lump grainstones and packstones with burrows and molds of large megalodont pelecypods and *Worthenia* gastropods (Bosellini, 1965, 1967). Thick subtidal units are capped by either (a) tepee structures (0.25–2 m thick) that consist of one to three thin diagenetic cycles which collectively have been disrupted into tepees or (b) red, massive, soil-like breccias of variable thickness (0.20–1.0 m thick).

Analogous to the tepees of the Latemar buildup, the Dolomia Principale tepees occur as low-relief antiforms with vadose cements, pisoids, and pisolitic breccias, testifying that the tepees are primarily the result of complex vadose diagenetic alteration of very thin (10–35 cm thick) preexisting cycles stacked at the top of a thick basal cycle.

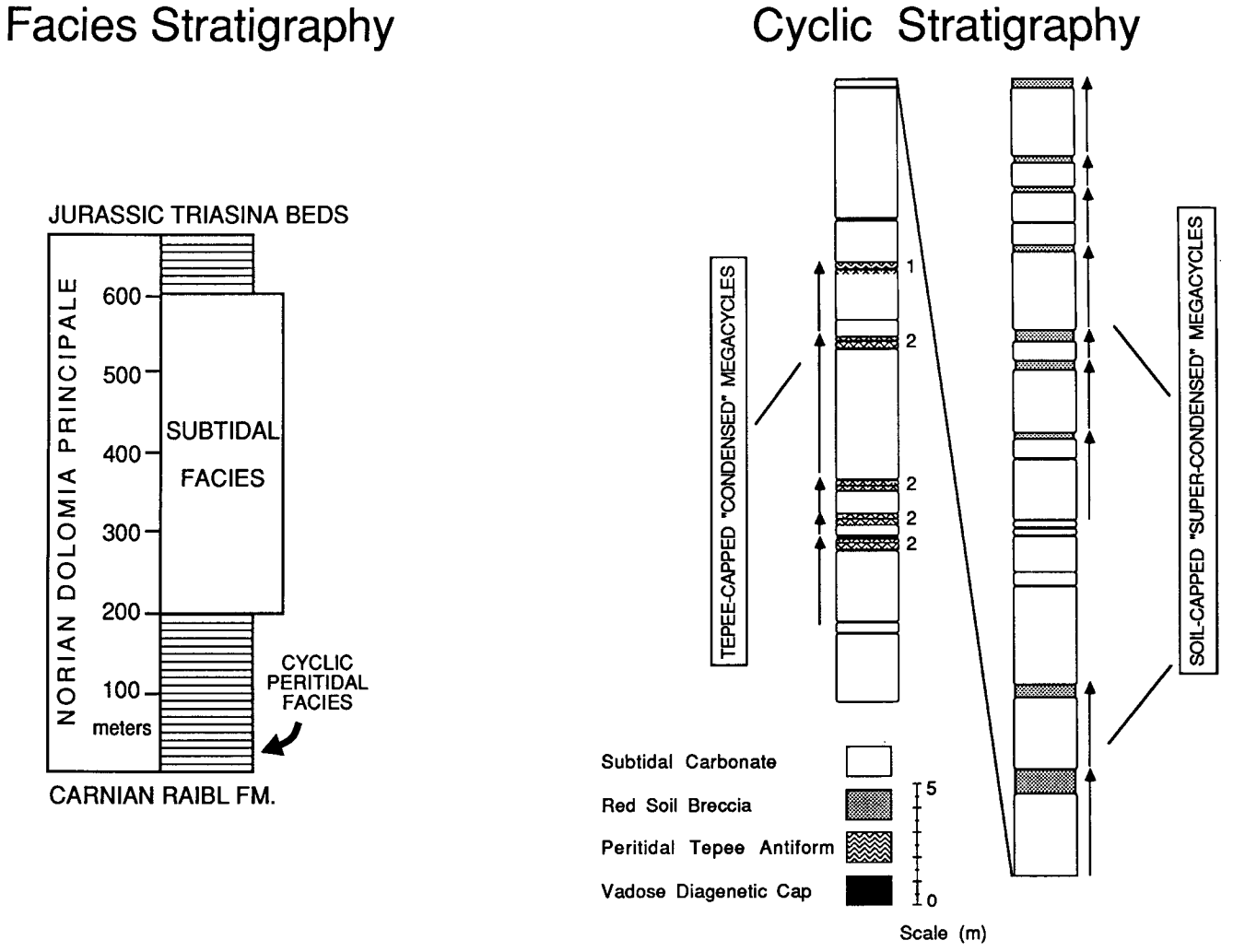

Figure 15. Facies stratigraphy and cyclic stratigraphy of the Norian Dolomia Principale in the Dolomites region of northern Italy. Facies stratigraphy shown in column on left. The measured section (on the right) of the "subtidal facies" of the Dolomia Principale displays a typical succession of meter-scale cycles with vadose diagenetic caps, tepee caps, and soil caps. Meter-scale fifth-order cycles are grouped into tepee-capped, "condensed" fourth-order megacycles and soil-capped, "super-condensed" fourth-order megacycles.

The red soil-like breccias occur only on top of thick subtidal units that lack caps of thin-bedded diagenetic cycles disrupted into tepees. The red breccias are analogous to the red soil-like breccias observed in the Loferite cycles (Fischer, 1964; see below) and in Pleistocene examples from south Florida (Perkins, 1977) and Bermuda (Ruhe and others, 1961; Land and others, 1967). The Dolomia Principale examples incorporate centimeter-scale clasts derived from underlying subtidal units and display very irregular lower boundaries with matrix-filled pipes (dissolution pipes?) penetrating the upper 0.5 m or so of some of the underlying thick subtidal units.

At Passo di Fittanze above Ala in the Adige Valley, there is a continuous road-cut exposure (several hundred meters of vertical section) that was a target for our study. We measured in detail a 55-m-thick section that we consider representative of the subtidal facies of the Dolomia Principale in this part of the Southern Alps. It displays both types of diagenetic cycles in fresh outcrop (Fig. 15), where individual fifth-order diagenetic cycles are seen to be grouped into thinning upward, tepee-capped megacycles or occur as solitary subtidal units topped by red soil zones.

By analogy with the tepee-capped megacycles of the Latemar tepee facies, the thick cycles capped by tepee zones in the Dolomia Principale are considered to represent "condensed megacycles" that have missed one or more of the fifth-order cycle-producing beats on the falling limb of an asymmetric fourth-order wave. The incomplete thinning-upward megacycles of the Dolomia Principale argue for composite, glacio-eustatic sea-level rhythms with Milankovitchian characteristics, similar to those that were operating during the Ladinian (see above). Most of the Dolomia Principale condensed megacycles consist of thinning-upward bundles of three, which in light of a Milankovitchian composite five-to-one ratio of superimposed orders of eustasy, suggests that on average, two beats of fifth-order sea level per megacycle failed to produce a cycle, resulting in prolonged subaerial exposure and tepee formation.

The thicker diagenetic cycles of the Dolomia Principale, which are capped by the red, soil-like breccias, are interpreted to record extended periods of subaerial exposure and vadose diagenesis, much longer than that required to form the thin (10 cm thick) caliche crust that normally caps the Dolomia Principale subtidal cycles (Hardie and others, 1986). The red

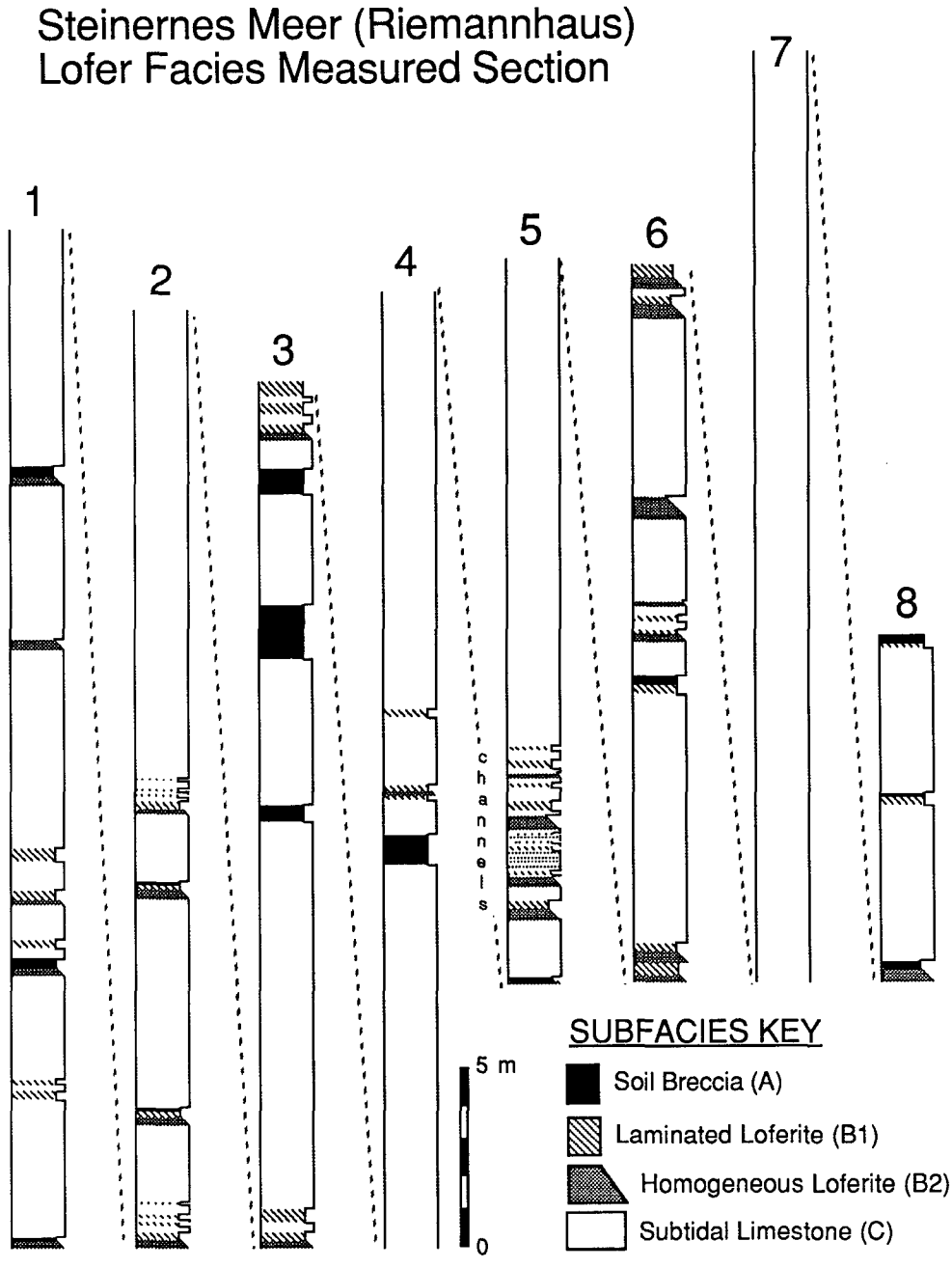

Figure 16. Measured section of the Norian Lofer facies of the Dachsteinkalk at the Steinernes Meer, Austria. Section was measured in the cirque near the Riemannhaus (see Fischer, 1964). Section begins at base of column 1 and ends at top of column 8. See text for descriptions of individual subfacies.

soils occur only on top of single thick subtidal units that lack caps of thin diagenetic cycles. As suggested by Hardie and others (1986, p. 452), tepees may form only where appropriate indurated thin layers (that is, thin cycles) already exist at the exposed surface. If such is the case, then the difference between thick subtidal units with tepee caps (that is, condensed megacycles) and the red soil-like caps may be related more to differences in preceding sea-level history than to differences in climatic conditions during exposure periods (Hardie and others, 1986).

We interpret the thick cycles with red soil-like caps as "condensed megacycles," but in contrast to the tepee-capped condensed megacycles, the degree of stratigraphic condensation is more pronounced. Instead of missing one or two beats of potentially cycle-producing fifth-order sea level within the composite fourth- and fifth-order arrangement, all but one of the fifth-order beats failed to yield a cycle. In this interpretation, then, soil-like caps represent as many as 4 missed beats of fifth-order eustasy per composite megacycle, when sea level oscillated beneath the top of the platform for roughly 80% of the megacycle duration.

The Ala measured section displays a systematic vertical variation in the two varieties of condensed megacycles. The lower half of the section consists primarily of tepee-capped megacycles ("normal" condensed megacycles), whereas the upper half of the section is marked primarily by red-soil–capped megacycles ("super" condensed megacycles). The thickness of the megacycles remains more or less uniform (ranging from 1–4 m), regardless of the type of cap, be it a tepee or red soil-like breccia. We suggest that the overall variation in megacycle style, from tepee-capped to soil-capped, is a systematic succession of megacycle variability related to long-term, third-order change in relative sea level, specifically a slow decrease in third-order accommodation. Thus, as third-order sea level de-

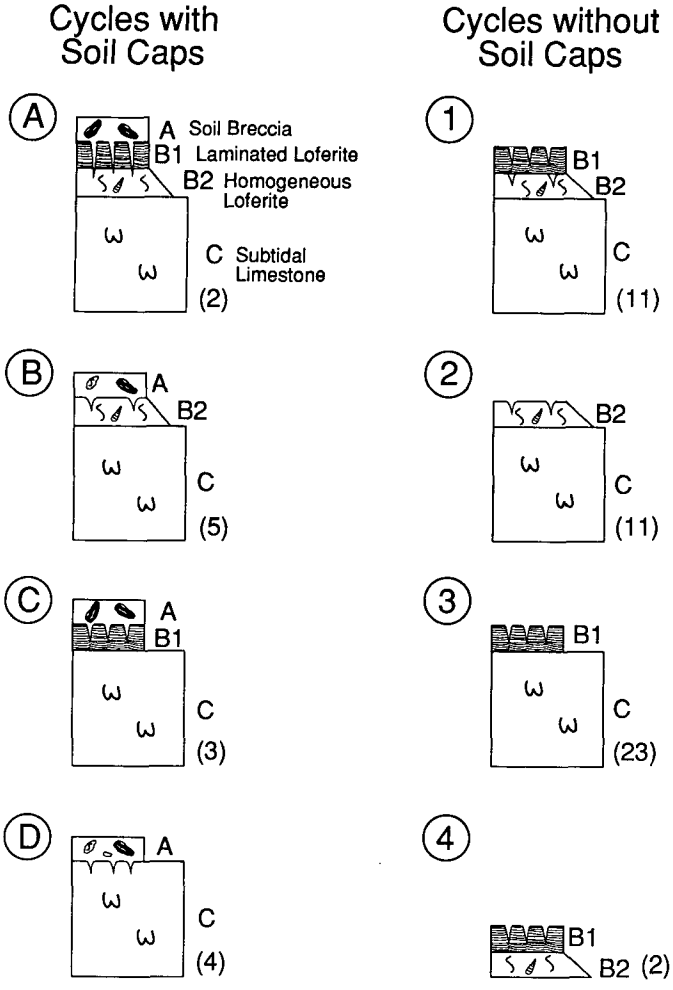

Figure 17A. Schematic representation of disconformity-bounded Lofer cycle types found at Steinernes Meer. Numbers in parentheses refer to number of cycles of that type in the section. All cycles show evidence of upward shoaling. See text for descriptions of subfacies.

Trailing Unit

Leading Unit	C	B2	B1	A
C	--	29	26	4
B2	11	--	15	5
B1	34	2	--	5
A	14	0	0	--

Figure 17B. Matrix of stacking patterns of Lofer subfacies. Note the lack of deepening-upward subfacies pairs. Laminites (subfacies B1) never occur on top of soils (subfacies A).

creased, the platform top experienced progressively reduced space for deposition, forcing each fourth-order megacycle to systematically miss more fifth-order beats and become progressively more condensed. Here again, a critical step in the link from small cycles to larger sequences is achieved through an appreciation of cycle stacking patterns, interpreted with Sander's Rule in mind.

The Lofer Facies of the Dachsteinkalk: A Complex Cyclic Stratigraphy Influenced by Tectonic Pulses. The Norian Lofer facies of the Dachsteinkalk of the Northern Limestone Alps (Fischer, 1964) is widely used as a reference example of meter-scale cycles produced by high-frequency sea-level oscillations. Fischer's (1964) outstanding descriptions of the major rock types of the Lofer facies, which served as the foundation for his original ideas on carbonate cyclicity, remain unsurpassed. Our re-examination of the Lofer facies focused on (1) the internal stacking patterns of lithologic members (or subfacies) within disconformity-bounded cycles, (2) megacycles and their stratigraphic arrangement, and (3) possible mechanisms responsible for Lofer cyclicity.

In terms of the subfacies (as defined by Hardie and Shinn, 1986), we recognized four basic types within the Steinernes Meer section.

(1) Subfacies C—Limestones consisting of <1- to 26-m-thick beds of wackestones to grainstones with submarine hardgrounds; a rich fauna including abundant megalodont pelecypods (Fischer, 1964; member C, "megalodont limestone").

(2) Subfacies B2—Dolomitic, burrowed, peloidal wackestones and packstones with a restricted fauna of thin-shelled gastropods and ostracods that may show prism cracks (Fischer, 1964; member B, "pellet and homogeneous loferites").

(3) Subfacies B1—Dolomitic laminite commonly containing prism and sheet cracks, crinkled laminae, and shrinkage pores (Fischer, 1964; member B, "algal mat loferite").

(4) Subfacies A—Intraformational conglomerate commonly containing clasts of the other subfacies in a green, brown, or red argillaceous matrix (Fischer, 1964; member A).

Fischer (1964) convincingly interpreted subfacies C to be a subtidal deposit, subfacies B2 and B1 to be intertidal in origin, and subfacies A to be a soil related to subaerial exposure. He made a case for sea-level oscillations as the predominant factor controlling the repeated alternation of subtidal and intertidal/supratidal deposits. In particular, he interpreted the "Lofer cycle" as a transgressive allocycle in which basal intertidal-supratidal fenestral laminites ("loferites") pass upward into megalodont-bearing subtidal units, recording a sea-level rise and a transgression of the shoreline. In turn, soils cap the subtidal member, marking a sea-level fall and the completion of a 10^4-yr cycle, possibly driven by the Milankovitch obliquity rhythm (Fischer, 1964, 1975). This transgressive "Lofer cycle" model did not fit with our own findings for Norian carbonates from the Southern Alps. In an effort to resolve this apparent conflict, we examined Fischer's (1964) Austrian Steinernes Meer and Dachstein sections as well as the Kehlstein outcrops above Berchtesgaden, West Germany, seeking comparisons with the Norian Dolomia Principale of the Southern Alps.

At Steinernes Meer, we measured a 192-m-thick, unbroken section consisting of 61 disconformity-bounded cycles (Fig. 16). Our preliminary finding is that the Lofer cycles are in fact regressive and are closely analogous to the Dolomia Principale cycles; that is, where soils occur, they are located on top of subtidal units (as in the subtidal facies of the Dolomia Principale) or on top of laminites (as in the peritidal facies of the Dolomia Principale; Bosellini and Hardie, 1985). We found no examples of soils overlain by intact laminites. Indeed, Fischer's published section from the Steinernes Meer bears out our observations (see Fischer, 1975, Fig. 27-1).

The transgressive Lofer cycle model was largely based on the Dachstein Lofer section (Fischer, 1964, Fig. 3; 1988, personal commun.), which contains several soils overlain by laminite subfacies. Field evidence at the Dachstein section is somewhat equivocal, however. In several instances, what appeared to be intact laminites above soils were traced laterally into soil zones that clearly had incorporated large tiles of dolomitic laminite. Even if these equivocal examples are taken to be transgressive cycles, there remains a clear preponderance of shallowing-upward cycles even in the Dachstein Range Lofer facies. Haas (1982) and Schwarzacher and Haas (1986) have also observed a predominance of regressive cycles in the Lofer equivalent in Hungary; however, Haas (1982) observed 12 different stacking patterns of subfacies within disconformity-bounded cycles, several of which recorded both flooding and shallowing phases of relative sea-level change (Haas, 1982, Fig. 1). The presence of deepening-upward cycles in

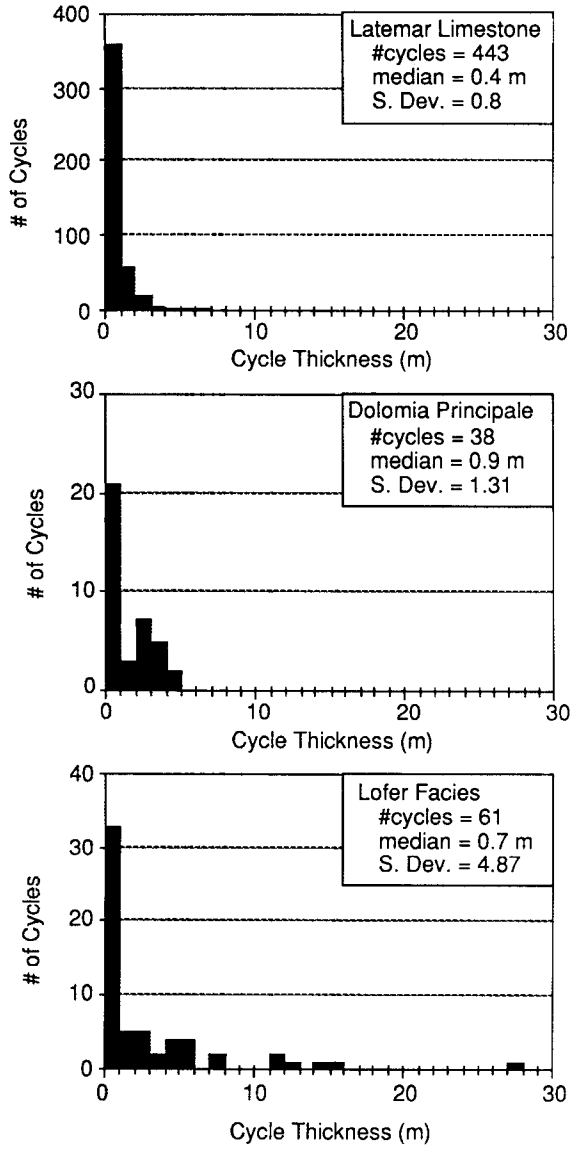

Figure 18. Statistical summary of cycle thicknesses from the Ladinian Latemar platform, the Norian Dolomia Principale at Ala Avio, and the Norian Lofer facies at Steinernes Meer. Lofer cycles show the widest range in thickness, followed by the Dolomia Principale and the Latemar. This wide range of thicknesses at the Steinernes Meer is interpreted to be the result of the addition of a strong tectonic component that acted with a highly variable magnitude.

the Lofer facies cannot be ruled out, but at this point, it is certain that they are the exception rather than the rule.

Our study of the Steinernes Meer section and other Lofer facies localities has provided additional information about the nature and origins of cyclic deposition in these carbonates. The 61 cycles measured at the Steinernes Meer section can be grouped into 2 classes, based on the presence or absence of soil horizons at their upper boundary. The cycles can be further characterized by the vertical succession of the four main subfacies as observed in the field, as illustrated in Figure 17A. Figure 17B is a matrix that summarizes the vertical stacking patterns of the subfacies at the Steinernes Meer section. The data in Figure 17 reveal several important features of the internal ordering of cycle components.

(1) Soils were found on top of all types of subfacies. The lower boundary of a soil zone relates to the degree of reworking at each horizon. In most cases where soils were developed directly on the megalodont limestones, centimeter-scale clasts of the intertidal subfacies were also incorporated in the soil matrix, indicating the complete reworking of a pre-existing peritidal cycle cap. Thus, they cannot be considered "diagenetic cycles" in the sense of the Latemar platform or the subtidal facies of the Dolomia Principale, where subaerial diagenesis was superimposed directly on subtidal sediments.

(2) Only subtidal units follow soil horizons. Subtidal units directly overlying soils record the drowning of the platform without significant deposition until water depths were sufficient for wholly subtidal deposition. This is consistent with the "lag depth" concept inferred from modern analogues (R. N. Ginsburg, 1971, personal commun.; Hardie and Shinn, 1986) and the other Triassic sections examined in this study.

(3) Laminated loferites (subfacies B1) are rarely succeeded by homogeneous loferites (subfacies B2), whereas the reverse is commonly the case. Preservation of layering and abundant desiccation features in the laminated loferites is indicative of an upper supratidal depositional environment, whereas the burrowed homogeneous loferites with their restricted fauna are more analogous to burrowed carbonate muds in modern restricted intertidal ponds (Hardie, 1977). The predominance of the B2–B1 subfacies stacking order (that is, B2 overlain by B1) over the B1–B2 sequence reflects the dominance of regressive sequences associated with tidal-flat aggradation and progradation (compare with Hardie and Ginsburg, 1977, Fig. 67).

(4) Many cycles (23 out of 61) consist solely of C–B1 subfacies couplets. The high frequency of C–B1 subfacies couplets (lacking subfacies B2 transitions) may reflect the patchy lateral distribution of intertidal ponds. The local paleotopography may have exerted a major control on the subfacies-scale stratigraphic record for a given stratigraphic section (Hardie, 1977).

(5) Most cycles (47 out of 61) are capped by either laminated loferites (36 out of 61) or homogeneous loferites (11 out of 61). If one assumes that the soils probably represent longer periods of subaerial exposure than do the loferites, it follows that the duration (and magnitude?) of relative sea-level fall during soil formation was much greater than normal. Loferite caps perhaps represent the abandonment of tidal flats after progradation, whereas the less numerous soils mark significant changes in relative sea level.

Lofer cycles measured at the Steinernes Meer section have a wide range of thicknesses when compared to the Latemar or Dolomia Principale cycle populations (Fig. 18). At Steinernes Meer, decameter-scale subtidal beds punctuate the record at random intervals (Fig. 19). These massive units commonly contain submarine hardgrounds and distinct zones characterized by faunal changes indicating fluctuations in the conditions of the subtidal environment. It is possible that the unusually thick cycles are, in fact, amalgamated megacycles in which high-frequency sea-level oscillations may be recorded as omission/cementation surfaces or as variations in faunal content. A more detailed investigation of the internal stratigraphies of these anomalous units is required to evaluate this hypothesis.

Extremely thin cycles are also common in the Steinernes Meer section (Fig. 18). A cluster of centimeter-scale units (predominantly C–B1 and C–B2 subfacies couplets) occupies the middle of the section (Figs. 16 and 19). This complex of thin units is cut by small tidal channels with about 2 m in relief. The paleogeography of the Dachstein shelf was clearly more complex than at the small, atoll-like Latemar. Lateral transport of sediment must have been a factor in the development of the Lofer facies, as it is with modern progradational tidal flats (Hardie and Shinn, 1986). The striking similarity of the Lofer facies, with its laminite caps, restricted

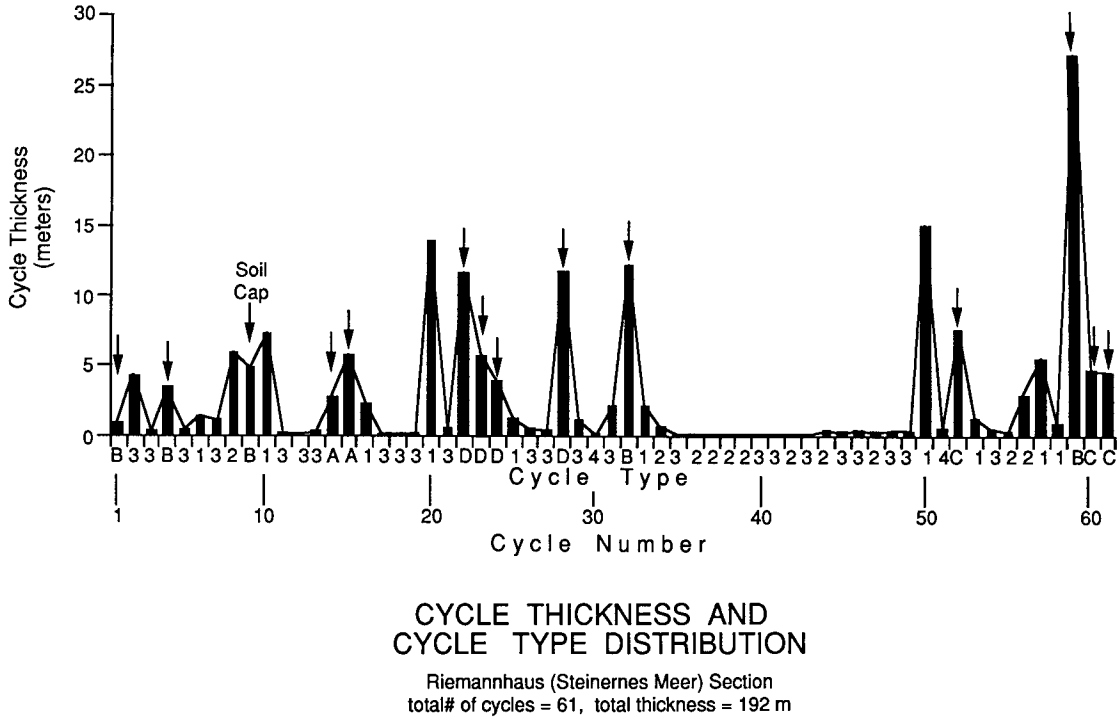

Figure 19. Graphical representation of measured section of the Lofer facies at Steinernes Meer, showing the stratigraphic succession of cycle thicknesses arrayed from bottom (left edge of graph) to top of section (right). Arrows mark cycles that have soil caps. Soils are distributed throughout section and generally cap thicker-than-average cycles. Cycle type codes refer to subfacies stacking patterns within disconformity-bounded cycles (see Fig. 17A). Cycle numbers index cycles from number 1 at the base of the section to number 61 at the top. Thinning-upward (toward the right) groups of cycles occur (that is, cycles numbered 22–27, 28–30, 31–35, 52–55) but contain a variable number of individual cycles.

intertidal subfacies, and meter-scale channels, to modern progradational carbonate tidal flats (see Hardie and Ginsburg, 1977) raises the possibility of lateral transport of sediment from subtidal to supratidal environments as a cycle-producing mechanism (Ginsburg, 1971; Hardie and Shinn, 1986). Autocyclicity thus must be added to the list as another mechanism that may have influenced deposition on the Dachstein shelf.

Deciphering the possible role of missed beats in the deposition of the Lofer facies is further complicated by the scarcity of well-defined fourth-order megacycles within the third-order sequence. Repeated thinning-upward packages, which are the fingerprints of high-frequency composite sea-level oscillation, are largely absent from the Steinernes Meer section. Groups of thinning-upward megacycles do occur (see cycles 22–35, Fig. 19), but they are sporadically distributed in the section as a whole and incorporate a variable number of individual cycles. These megacycles are not five-part packages, and we were unable to find Milankovitchian rhythms in our preliminary measured sections, using high-resolution spectral analysis of cycle thickness data (method of Hinnov and Goldhammer, 1988; compare also the inconclusive results of Schwarzacher and Haas, 1986, using Walsh functions on the Hungarian Lofer data).

The random stratigraphic distribution of cycle types and cycle thicknesses in the Steinernes Meer section radically departs from the systematic arrangement of cycles seen at the Latemar or the smooth gradation of subaerial exposure features observed at the Ala section. At Steinernes Meer, no large-scale trends in cycle thickness can be seen, and soils are found scattered throughout the section (Figs. 16 and 19). Although there is no obvious pattern in their stratigraphic distribution, soil breccias were found only capping cycles of average to greater-than-average thickness, indicating a connection between the formation of "over-thickened cycles" and prolonged subaerial exposure. This relationship stands in direct contrast to the Latemar's systematic succession, where thin cycles are linked to increased subaerial exposure.

Both eustatic and tectonic engines could be invoked to explain the range of Lofer cycle types and the anomalous juxtaposition of thick cycles and soils seen at the Steinernes Meer. The eustatic "missed beat" record of the Pleistocene of southern Florida with thick, amalgamated subtidal cycles separated by unconformities of substantial duration provides one possible analogue for the soil-capped Lofer cycles (Perkins, 1977). This explanation would require the 10^5-yr sea level to be a response to the dynamics of large polar ice caps that would swamp any higher-frequency oscillations; however, the Triassic was not a time of major glaciation with polar caps the magnitude of those of the Pleistocene (Crowell, 1982).

The lack of cycle thickness rhythms, the irregular distribution of anomalously thick cycles (amalgamated megacycles?), and the wide range and irregular stratigraphic distribution of subaerial exposure types suggest that factors in addition to (in lieu of?) rhythmic composite sea-level changes were an important influence on cyclic sedimentation. Tectonic forcing of Lofer cyclicity has been suggested by Cisne (1986). Stepwise subsidence with periods of rapid slip alternating with periods of quiescence, slow subsidence, or even uplift would produce a wide array of cycle thicknesses and explain the enigmatic pairing of thick subtidal units and soils.

We suggest that Lofer facies deposition was in large measure controlled by short-term variations in subsidence rate, leading to a chaotic stratigraphic distribution of cycle thicknesses and diagenetic features. There are no discernible megacycle patterns with Milankovitchian (or any other rhythmic forcing) origins. On a larger scale, there are no stratigraphic patterns suggestive of third-order sea-level control. These negative conclusions, arising as they do from perhaps the world's most famous "rhythmic carbonate," should serve as a warning to searchers for stratigraphic rhythms. Complex stratigraphies, such as that of the Steinernes Meer,

probably record the nonrhythmic sum of pulses of subsidence, sedimentation, autocyclicity, and sea-level variation. Such nonrhythmic records appear to dominate the stratigraphic column, and what insight we may gain as to their origins will probably be achieved through the use of stratigraphic patterns recognized from simpler depositional systems, such as the Ladinian Latemar buildup.

DISCUSSION

Cycle Stacking Patterns of the Latemar Buildup and Some General Principles

The style of vertical changes in cycle stacking patterns depicted by the systematic succession of amalgamated megacycles (submergence dominated) to rhythmic megacycles (submergence ~emergence) to condensed megacycles (emergence dominated) and then back to rhythmic megacycles displayed by the Latemar succession can be summarized with a computer simulation using a fifth/fourth-order composite wave superimposed on a third-order wave, under conditions of constant platform sedimentation and long-term subsidence. The simulated sea-level–subsidence–sedimentation history is shown in Figure 20. For this run, the rate of third-order eustatic fall is less than the rate of background platform subsidence (run data are summarized in the caption of Fig. 20). The resultant simulated stratigraphy, displayed in Figure 20, is remarkably similar, although on a reduced scale, to the cyclic stratigraphy of the Latemar, shown in Figure 21. The simulation demonstrates the manner in which high-frequency cycles (fourth and fifth order) systematically change their stacking patterns (that is, their thicknesses, subfacies characteristics, and early diagenetic attributes) across a third-order sequence owing to systematic changes in accumulation space available during one complete third-order sea-level change. As third-order sea level rises, the superimposed high-frequency oscillations are forced to miss subaerial exposure beats because of the net increase in mean water depth, resulting in amalgamated megacycles with thickened subtidal units. Higher-frequency cycles and megacycles are relatively thick and submergence-dominated in character (that is, deepest subtidal facies, prone to early submarine diagenesis). In contrast, third-order sea-level fall produces a net shallowing, so that submergence beats of the high-frequency oscillations are now commonly missed, resulting in condensed megacycles with soil or tepee caps. Higher-frequency cycles and megacycles are relatively thin and emergence dominated (that is, shallowest subtidal facies, prone to early vadose diagenesis). At the crest and the trough of the third-order cycle conditions are just right to produce five-part rhythmic megacycles ("Goldilocks window"). Higher-frequency cycles and megacycles are of intermediate thickness in comparison to underlying and overlying strata, and the proportion of submergence time to emergence time is roughly equivalent. This "generic" third-order sequence is thus characterized by a systematic vertical change in cycle and megacycle stacking patterns (that is, thinning and thickening) accompanied by a systematic change in submergence-dominated versus emergence-dominated cycles and megacycles, precisely analogous to the pattern observed at the Latemar (Fig. 21). It is these systematic changes in fourth- and fifth-order cycle thicknesses that generate the relative rises and falls in the long-term Fischer plot (Fig. 9).

The particular example shown here in Figure 20 is based on composite sea-level changes, but we have achieved comparable fourth-order autocyclic systematic changes using both depth-dependent sedimentation and lag-depth–dependent depositional mechanisms (that is, no built-in fourth-order eustatic fluctuation) superimposed on third-order relative sea-level changes (Fig. 22). In Figure 22, we illustrate two stratigraphic simulations and their respective subsidence–sedimentation–sea-level records. The simulation on the left-hand side of the diagram displays high-frequency fourth-order autocycles that were generated by simply superimposing a third-order oscillation (period = 1 m.y., amplitude = 5 m) on top of a platform subsiding at a linear rate equal to 5 cm/1,000 yr. Sedimentation rate was fixed at 10 cm/1,000 yr, and a lag depth of 2 m was used. No higher-frequency fourth- or fifth-order sea level was added. The generation of fourth-order cycles (31 cycles, average 96,354 yr/cycle, average 4.8 m/cycle) was dictated by the interaction of long-term accommodation space (third-order sea level plus subsidence) and lag depth. When accommodation space exceeds lag depth, sedimentation ensues and the platform aggrades vertically until it intersects the trace of third-order sea level, at which point it is briefly exposed (forming a very thin diagenetic cap). At this point, sedimentation ceases until the requisite accommodation space is created to overcome lag depth. In this manner, high-frequency fourth-order cycles are generated in the absence of high-frequency fourth-order eustasy. Most significant is the fact that the fourth-order cycles display a systematic vertical stacking pattern of thinning and thickening in response to long-term, third-order eustasy. Thus, the development of a systematic succession of cycle stacking patterns need not necessarily be directly attributed to high-frequency allocycles only. The simulation on the right-hand side of the diagram (Fig. 22) shows high-frequency fourth-order allocycles that were generated by superimposing high-frequency, fourth-order eustasy (period = 100,000 yr, amplitude = 5 m) on top of a third-order oscillation identical to that used in generating the autocycles (period = 1 m.y., amplitude = 5 m). Values of subsidence, sedimentation rate, and lag depth are also identical to those utilized in the autocycle simulation. The fourth-order allocycles are nearly identical to the autocycles (30 cycles, average 98,566 yr/cycle, average 4.9 m/cycle) and display a very similar systematic vertical stacking pattern of thickening and thinning in response to third-order forcing. What is clear in both examples, reinforcing the message provided by the Latemar stratigraphy, is the fact that the long-term, third-order signal is not dependent on the nature of the high-frequency cycle-generating mechanism.

What is very instructive is the fact that the autocycles in Figure 22 have an average periodicity that not only falls within the "Milankovitch band" but approximates the short eccentricity cycle, despite the fact that there was no Milankovitchian input. This reinforces the notion that calculation of average cycle periodicity can in no way be used as unequivocal evidence for or against Milankovitch forcing (Hardie and Shinn, 1986; Goldhammer and others, 1987; Algeo and Wilkinson, 1988). What is equally as interesting is the fact that cycle thickness does not reflect cycle duration or periodicity. For example, in the autocyclic run, cycle 2 (top at 151,000 yr) took 102,000 yr to form, and cycle 7 (top at 632,000 yr), which is much thinner, took 123,000 yr to form. Also intriguing in the autocycle simulation is the fact that despite constant lag depth, *lag time* (that is, the time it takes for sedimentation to resume following exposure and the subsequent flooding of the platform; Read and others, 1986) varies throughout the simulation for each successive cycle. We suggest that lag time should and will vary throughout long-term stratigraphic development and that artificially fixing lag time at a constant value (for example, Read and others, 1986) is unwarranted.

The Hierarchy of Stratigraphic Forcing

As pointed out by Wilson (1975) and Kendall and Schlager (1981), a hierarchy of relative changes in sea level and cyclic sedimentation, independent of local tectonics, is a fundamental theme that emerges from consideration of marine carbonate deposits throughout the geologic record. These concepts are not novel and can be traced back to Suess (1888) and Grabau (1913), who, among others, recognized that stratigraphic

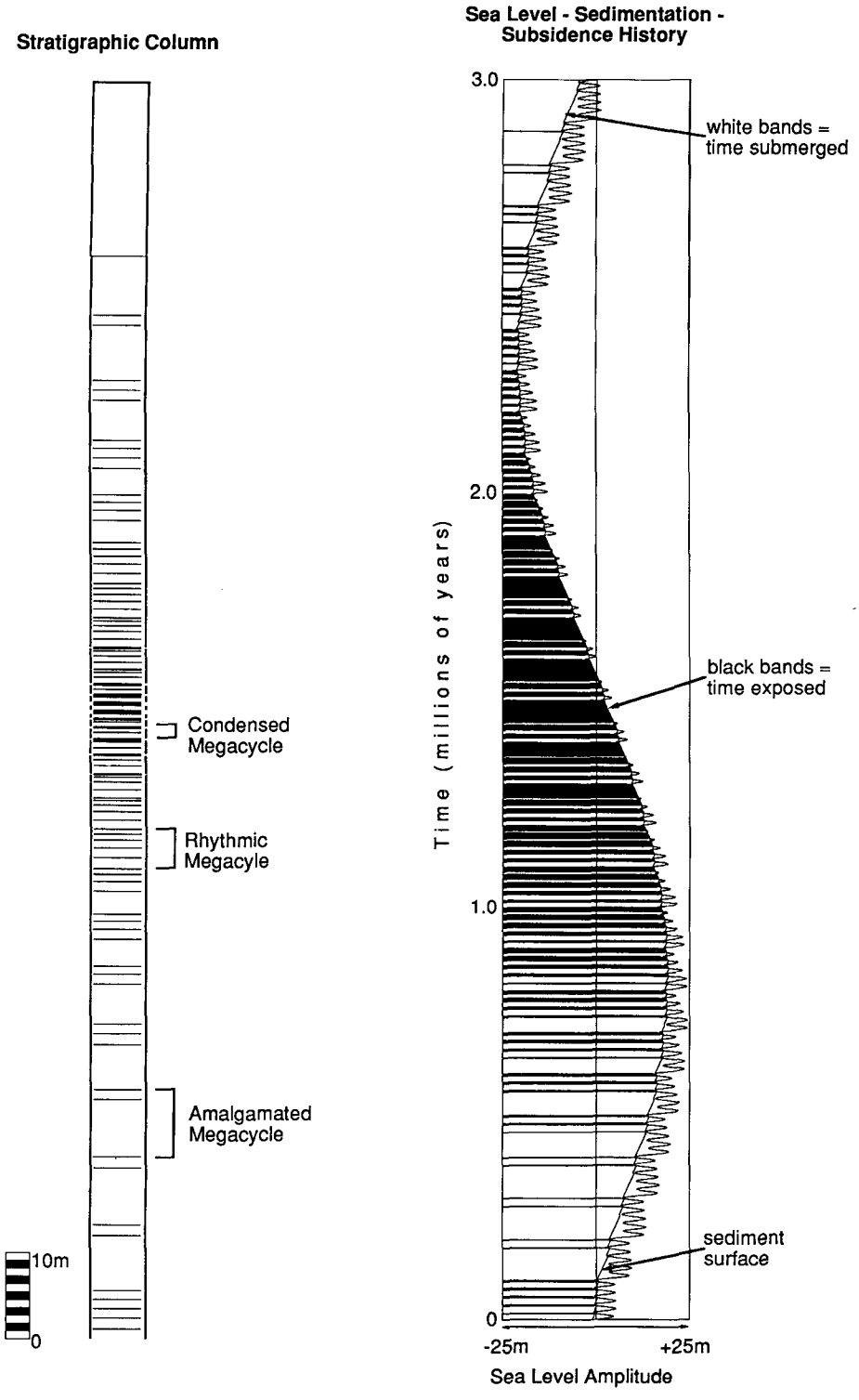

Figure 20. Simulation of the submergence-emergence record on a carbonate platform of composite high-frequency sea-level oscillations (20,000-yr amplitude > 100,000-yr amplitude) when superimposed on a third-order (3 m.y.) sea-level change, using the "Mr. Sediment" computer program. Resulting cyclostratigraphy is shown on the left of the figure. On the third-order rise, some of the high-frequency "beats" fail to expose the platform top resulting in the deposition of a "missed beat" stratigraphy of amalgamated megacycles. On the third-order fall, "missed beats" result from failure of some of the high-frequency oscillations to flood the platform, producing condensed megacycles. At the crests and troughs of the third-order curve, the conditions are just right for submergence and emergence of the platform with every successive high-frequency oscillation, resulting in rhythmic megacycles ("Goldilocks" megacycles). Input data: sedimentation rate = 0.1 m/1,000 yr; subsidence rate = 0.05 m/1,000 yr; sinusoidal 20,000-yr wave with 3-m amplitude; asymmetrical 100,000-yr wave with 2-m amplitude; third-order wave with 40-m amplitude and 3-m.y. duration.

cycles of differing orders of magnitude could be attributed in part to differing orders of eustasy. Barrell (1917) introduced the term "composite cycle" for systems in which cycles of differing wavelengths are superimposed upon each other. Relative fluctuations in sea level occur with different frequencies, yielding an ordered hierarchy of relative sea-level cycles based upon the temporal duration of the fluctuation (that is, third order, fourth order, and so on). This concept is now well established, as indicated by Exxon's global cycle charts constructed for the Phanerozoic (Vail and others, 1977; Haq and others, 1987), which show superimposed orders of stratigraphic and relative sea-level cycles interpreted to reflect eustasy (see Miall, 1984, p. 344–356, for a review of "cycles within cycles"). Significantly, different orders of relative sea-level change have characteristic amplitudes and rates of change (Donovan and Jones, 1979; Miall, 1984), reflecting the driving mechanism, be it glacio-eustatic (changing the amount of water in the basin) or tectono-eustatic (changing the shape and volume of the basin).

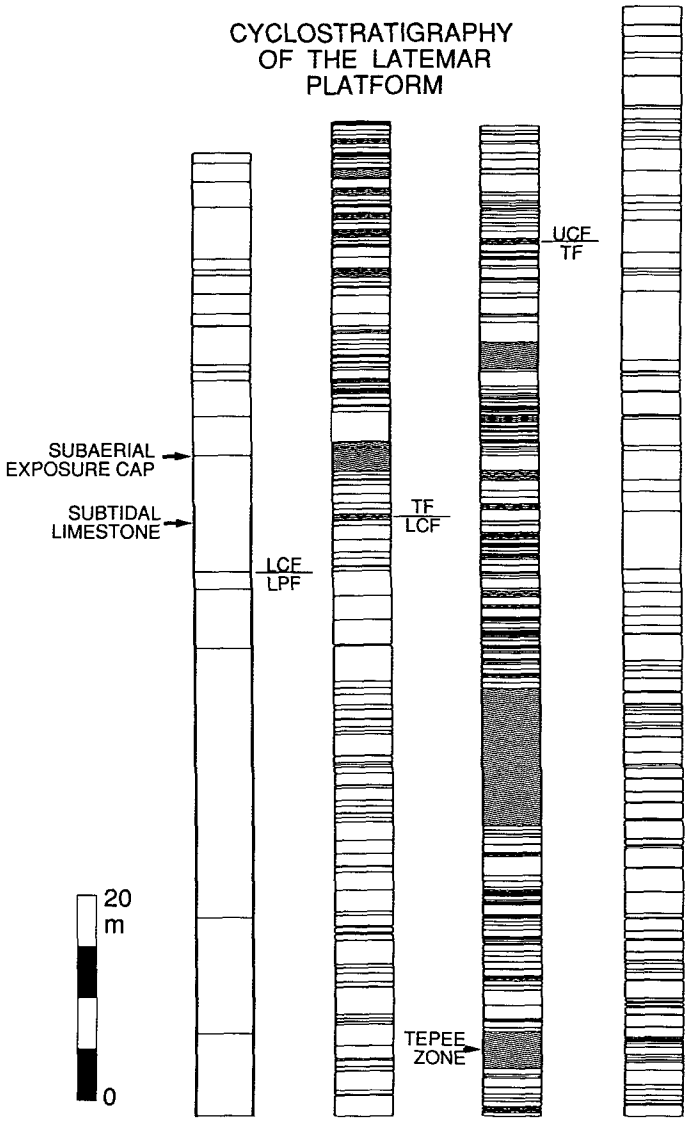

Figure 21. High-frequency cyclostratigraphy of the Latemar platform carbonates based on several measured sections correlated by lateral tracing of key cycles. This composite section includes the uppermost part of the lower platform facies (LPF), the complete lower cyclic facies (LCF), the complete tepee facies (TF), and the lower part of the upper cyclic facies (UCF). The stacking progression from amalgamated megacycles at the base (LPF) through rhythmic megacycles (LCF) to condensed megacycles (TF) and back to rhythmic megacycles (UCF) is well displayed in this approximately 200-m-thick section. Cycles and packages of cycles disrupted by tepees (tepee zones) are shown in zig-zag pattern. The thick tepee zone in the middle of the tepee facies is a 13-m-thick complex of tepee-capped cycles highly disrupted by multiple antiformal buckling and vadose cementation.

In consideration of the existence of superimposed orders of relative sea-level oscillations, we suggest that a hierarchy of stratigraphic forcing exists, which is largely dependent on the periodicity and relative amplitude ratio of superimposed relative sea-level fluctuations. In this hierarchical scheme, the lower-frequency sea-level cycles force the higher-frequency sea-level cycles, producing by this interaction a systematic internal architecture in the stack of higher-frequency depositional cycles, as illustrated in Figures 20, 21, and 22. For composite eustasy, this relationship follows from the empirical observation that the rates of change of the higher-frequency sea-level oscillations (fourth and fifth order) are typically much greater than those of the lower-frequency fluctuation (third order), owing principally to the differencs in their causative mechanisms, that is, glacio-eustasy for the fourth- and fifth-order changes but tectono-eustasy for the third-order changes (see Rona, 1973; Pitman, 1978; Donovan and Jones, 1979; Schlager, 1981; Miall, 1984; Haq and others, 1987).

The cyclostratigraphy of the Ladinian Latemar buildup provides an outstanding example of stratigraphic forcing by composite eustasy. As outlined above, the succession of amalgamated to rhythmic to condensed and back to rhythmic megacycles in the Latemar platform carbonates is the result of third-order forcing of fourth-order depositional megacycles. The forcing takes the form of a long-term systematic change in mean accumulation space, as third-order sea level rises and falls against a background of overall slow tectonic subsidence. On a smaller scale, the systematic upward thinning of the fifth-order depositional cycles within each fourth-order megacycle (Figs. 1 and 2) is also the result of a forcing hierarchy. In this case, the fourth-order sea-level oscillations have systematically changed the fifth-order accumulation space to force a thinning-upward succession of fifth-order depositional cycles. These are the basic thin couplets described in detail by Goldhammer and others (1987).

A different example is provided by the Lower Ordovician platform carbonates of the Appalachians (the Beekmantown and Knox Groups), where systematic variations in the stratigraphic stacking patterns of fourth-order peritidal cycles occur within third-order depositional sequences of 2–3 m.y. duration (Hardie, 1989; see also Nguyen and others, 1985; Hardie and Shinn, 1986) as revealed by Fischer diagrams (R. K. Goldhammer, unpub. data; Read and Goldhammer, 1988). This Lower Ordovician example is one of third-order forcing of a succession of *solitary* high-frequency fourth-order depositional cycles. With this type of cycle coupling, the effects of third-order forcing of higher-frequency cycles can be the same for both autocycles and allocycles, as the simulations illustrated in Figure 22 demonstrate.

A very different case of stratigraphic forcing is that of the Pleistocene carbonate platforms. During the Pleistocene, the fourth-order (~100,000 yr) sea-level oscillations were of exceedingly large amplitude (Fig. 3), so that they dominated the system to the point where the remaining orders of eustasy had little effect on the final stratigraphic output (see Fig. 6). We suggest that this pattern will be characteristic of all major glacial periods (the Pliocene-Pleistocene, the Permian-Carboniferous, and so on), owing in all probability, to the control on eustasy by the dynamics of growth and melting of large polar ice caps. During these major glacial periods, high-frequency glacio-eustatic sea-level oscillations with periodicities in the Milankovitch band (fourth and fifth order) will have large amplitudes relative to the lower-frequency fluctuations (second and third order) and will dominate the forcing system. With this type of high-frequency forcing, the impact of the lower-frequency change will be subdued, resulting in a stratigraphic record that may not contain evidence for a systematic hierarchy of stratigraphic forcing (see, for example, Heckel, 1986).

If our "generic" third-order sequence (Fig. 20) is a valid model for carbonate platform deposits other than the Latemar, then it has major implications for the use of fourth- and fifth-order cycle characteristics to identify third-order cycles in outcrops and cores of shallow-water carbonates, especially where stratigraphic control may be poor (Hardie, 1989). This would constitute a valuable bridge between cyclic stratigraphy at the meter scale and sequence stratigraphy at the seismic scale (see below). This

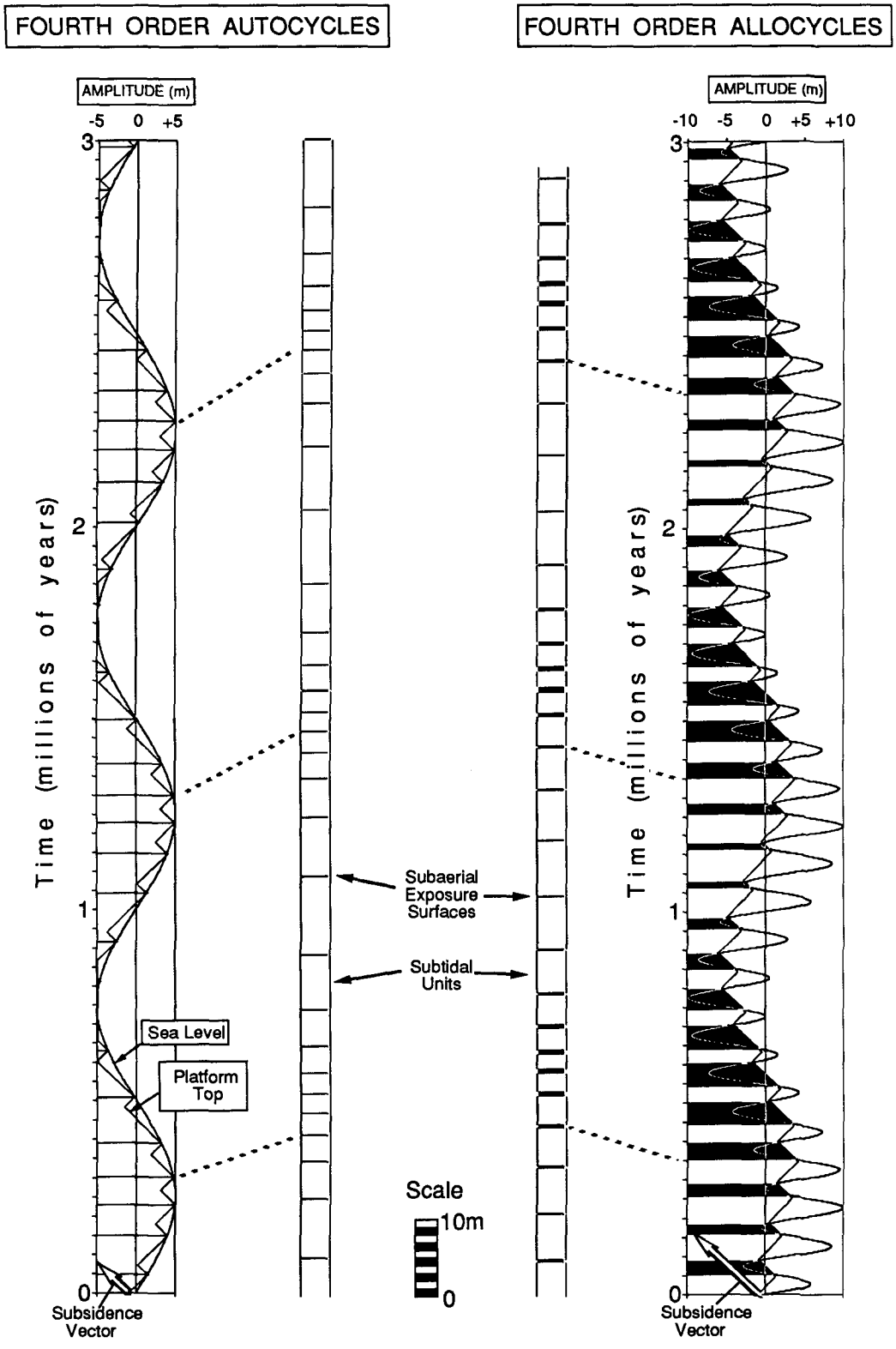

Figure 22. Comparative computer simulations of high-frequency, fourth-order autocycles versus allocycles. The record of autocyclic subsidence–sedimentation–sea-level interaction is illustrated to the left of the stratigraphic column with ages in thousands of years. Fourth-order autocycles are shown as white subtidal units that shallow upward to sea level; the supratidal cap is denoted by a thin black line. The record of allocyclic subsidence–sedimentation–sea-level history is displayed to the right of the stratigraphic column with ages in thousands of years. Fourth-order allocycles are shown as white subtidal units with thin, black subaerial exposure caps (ages in thousands of years).

model, however, also has major implications for the control of platform diagenesis by composite sea-level changes, and would, in particular, offer an explanation for the stratigraphic location in platform carbonate successions of early diagenetic realms, that is, intervals dominated by early marine diagenesis (hardgrounds, and so on) versus intervals characterized by early subaerial diagenesis (soils, peritidal tepees, and so on) (see below).

Sequence Stratigraphy and Systems Tract Development of the Latemar Buildup: The Link between Cyclic Stratigraphy, Facies Stratigraphy, and Sequence Stratigraphy

The Latemar sequences (sequence L1, L2, Fig. 8) provide an optimum stratigraphic framework for integrating the well-developed cyclic

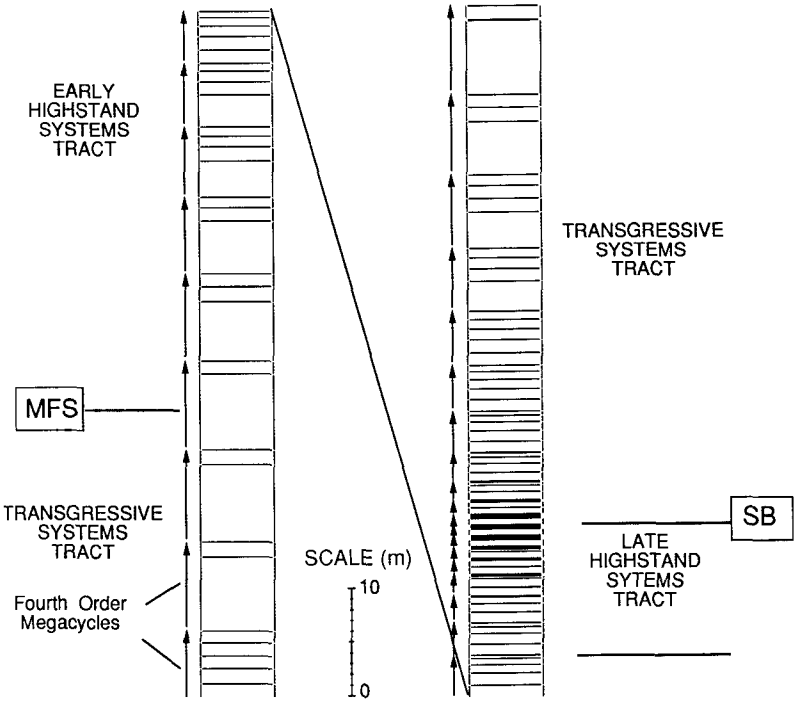

Figure 23. Interpretation of the systematic vertical succession of cycle and megacycle stacking patterns generated by sea-level–subsidence–sedimentation input shown in Figure 20 in terms of sequence stratigraphy. Fifth-order (meter-scale) cycles, consisting of a subtidal deposit (white) and a subaerial exposure cap (black), are grouped into fourth-order megacycles (vertical arrows to left of column). Megacycle boundaries on the stratigraphic column were picked from eustatic megacycle boundaries displayed in Figure 20. The simulated stratigraphy is subdivided into systems tracts based on stacking patterns of cycles and megacycles as well as changes in rates of third-order accommodation derived from Figure 20. MFS refers to maximum flooding surface, and SB refers to sequence boundary (see text). The thin depositional cycles at the base of the column are an artifact of the initial depth at the start of the run.

and facies stratigraphy of the Latemar succession (exposed in outcrop on a seismic scale) with the concepts of sequence stratigraphy (Vail and others, 1984; Vail, 1987; Van Wagoner and others, 1987; Sarg, 1989). This is significant because most analyses of basin stratigraphy utilizing sequence stratigraphy concepts focus primarily on the third-order–scale sequences (1–10 m.y. duration; a few to several hundred meters in thickness), and typically, seismic data cannot resolve the higher-frequency stratigraphic building blocks (that is, the fourth- and fifth-order stratigraphic cycles). Thus, the detail of the internal architecture of sequences and systems tracts is often unresolved (for example, Eberli and Ginsburg, 1989; Sarg, 1989). A depositional sequence may be defined as a conformable succession of genetically related strata bounded by interregional unconformities or their correlative conformities (that is, sequence boundaries; Mitchum and others, 1977; Van Wagoner and others, 1987). A depositional sequence is interpreted by Haq and others (1987) and Vail (1987) to be deposited during a third-order cycle of eustatic change in sea level starting and ending in the vicinity of the inflection points on the falling limbs of the third-order sea-level curve. A sequence can be subdivided into component systems tracts defined as a linkage of contemporaneous depositional systems (that is, shelf, slope, basin; Brown and Fisher, 1977), which are a three-dimensional assemblage of facies. Systems tracts, characterized by predictable large-scale geometry and facies associations, are defined according to position within a sequence, the types of bounding surfaces (type 1 or type 2 sequence boundaries, maximum flooding surface, and so on; see Van Wagoner and others, 1987, for a review of sequence stratigraphy nomenclature), and the stacking patterns of higher-frequency cycles (parasequences of Vail, 1987; Van Wagoner and others, 1987). As we have demonstrated (Figs. 20 and 22), the stacking patterns of high-frequency cycles (fourth and fifth order) aid in determining changes in long-term accommodation, and therefore, we can use the high-frequency cycle stacking patterns of third-order sequences to define the systems tracts of the sequence (Vail, 1987; Van Wagoner and others, 1987). This approach is especially critical in defining sequences and component systems tracts of many ancient carbonate platforms and shelves where large-scale, undeformed, two-dimensional geometries are typically lacking, or where seismic data are unavailable to complement other data sources (both subsurface and outcrop).

The connection between systems tracts and the stacking patterns of high-frequency cycles within third-order sequences in cyclic platform carbonates such as the Latemar is best exemplified by our computer simulation illustrated in Figure 20. In Figure 23, the cyclostratigraphy of our "generic" third-order sequence of Figure 20 has been interpreted in terms of sequence stratigraphy. In this "generic" third-order sequence, the simulation starts with flooding a carbonate platform that we arbitrarily assume was subaerially exposed for a significant amount of time (that is, bounded by an unconformity). The transgressive systems tract generated with third-order rise in sea level is characterized by a series of aggradational amalgamated megacycles. The maximum flooding surface (MFS), which caps the transgressive systems tract (Fig. 23), is placed at the time of maximum rate of long-term accommodation increase (Vail, 1987; Van Wagoner and others, 1987), which is defined quantitatively and dated by our combined sea-level–subsidence–sedimentation history (Fig. 20). Above the maximum flooding surface, the highstand systems tract is characterized by rhythmic megacycles (early highstand) that reflect a decline in the rate of third-order rise as the third-order wave crest is reached. This is followed by condensed megacycles (late highstand) that are a response to third-order sea-level fall, which now almost tracks subsidence. Overall, the fourth-order megacycles thin upward from the maximum flooding surface to the top of the sequence, owing to progressively declining third-order accommodation. The upper sequence boundary (SB) occurs within the interval of thinnest condensed megacycles and is placed at the time of maximum rate of long-term accommodation decrease. It is marked stratigraphically by the turnaround from fourth-order megacycles that progressively thin upward, to fourth-order megacycles that progressively thicken upward (Fig. 23). No erosion occurs and no lowstand deposit is formed on the platform top in our simulation, as the platform continues to experience repeated cycles of flooding and exposure. What is different is the enhanced subaerial exposure during each cycle as accommodation reaches a minimum at this stage (subsidence barely exceeds third-order sea-level fall)

(Fig. 20). Overlying the sequence boundary, the transgressive systems tract of the next sequence displays a series of thickening-upward fourth-order megacycles that proceed from condensed to rhythmic to amalgamated (Fig. 23). Thus, this sequence boundary is stratigraphically *transitional* without a basinward facies shift and is located entirely on the basis of stacking patterns of the higher-frequency fourth-order megacycles. There is no singular, long-term (that is, greater in duration than the period of a few fifth-order oscillations) erosional unconformity generated in the simulation because the rate of third-order sea-level fall is less than the rate of background platform subsidence. This sequence boundary cannot be a type 1 sequence boundary (rate of third-order fall > rate of platform subsidence at the shelf edge; Vail and others, 1984) but is more akin to a type 2 sequence boundary (rate of third-order fall < rate of platform subsidence at the shelf edge; Vail and others, 1984) that has, however, in this example, no updip correlative unconformity.

This type of sequence boundary with transitional instead of unconformable boundaries is found in the actual Latemar sequences (see below) and also is characteristic of the very thick Cambrian-Ordovician platform carbonates of the central Appalachians (Hardie, 1989). We suggest that this transitional type of sequence boundary will be a particular attribute of shallow-water carbonates because of the characteristic flat-topped geometry of most ancient and existing carbonate buildups. It is reasoned that with such flat-topped platforms, any slow third-order sea-level fall (that is, rate of fall < rate of subsidence) will be transmitted with equal effect across the entire, or almost entire, buildup. This, in turn, would allow the deposition of "conformity-bounded" sequences across the entire, or almost entire, buildup. Such conformity-bounded sequences would not be identified in seismic sections because of the lack of seismic discontinuities at their boundaries. It is also suggested that in some instances, conformity-bounded carbonate sequences may experience a rapid deepening with renewed third-order rise (relative or eustatic), and if the rate of rise is great enough, the platform may drown (Schlager, 1981; Kendall and Schlager, 1981). In these instances, a "drowning unconformity" (Schlager, 1989) with its condensed section will lie directly on a conformity-bounded sequence, which need not contain any evidence for subaerial erosion. Thus, both "conformity-bounded" sequences and "drowning-unconformity–bounded" sequences should be considered likely candidates to be encountered in the spectrum of carbonate sequence types, in addition to the type 1 and type 2 sequences (as defined by Vail and others, 1984; Van Wagoner and others, 1987) that are perhaps more readily recognizable because of their association with unconformities. We are mindful that such additions to the concept of sequences reach beyond the original definition that was developed from seismic stratigraphy, but as long as sequences remain genetically linked to third-order sea-level changes (Haq and others, 1987; Vail, 1987), then such additions to the concept are absolutely essential to avoid errors in reconstructing the geohistory of sea-level changes. For example, Haq and others (1987), relying on unconformities to identify third-order sequences, recognized only one sequence in the Ladinian section of the Dolomites, whereas we recognize two third-order sequences (Fig. 8, sequences L1 and L2) separated by a *transitional boundary* that records two significant third-order sea-level oscillations during Ladinian time.

The above considerations can now be used to interpret the basic elements of the sequence stratigraphy of the Anisian-Ladinian Latemar platform carbonates. Within the Latemar buildup, the first Latemar sequence (sequence L1, Fig. 8) is bounded at its base by an unconformity at the top of the middle Anisian Contrin Formation, characterized by meter-scale channels incised into the slope facies of the Contrin bank and infilled with slumped carbonate debris and megabreccias (most likely a type 1 sequence boundary; Harris, 1988). At the Latemar, the lowstand systems tract is represented only by the local submarine channeling and carbonate debris fill. Equivalent lowstand deposits in a more basinal setting (lowstand wedge, basin-floor fan, and so on) have not been recognized in and around the Latemar, presumably owing to the lack of a clastic source and the isolated nature of the Latemar. The transgressive systems tract of sequence L1 is represented by the lower platform facies, which formed in response to an increase in third-order accommodation (Fig. 9) largely the result of a eustatic third-order rise documented in other areas in addition to the Dolomites (Goldhammer and Harris, 1989). At the Latemar, as well as at the coeval Catinaccio buildup, the channeled interval atop the Contrin slope facies is immediately overlain by dark, laminated siliceous mudstone and pelagic carbonates of the Livinallongo Formation, recording the increase in accommodation associated with a rapid relative sea-level rise. Within the transgressive systems tract of the Latemar platform interior, subtidal depositional facies and abundant syndepositional marine diagenesis dominate the record, and fifth-order cycles are grouped into fourth-order amalgamated megacycles (Figs. 12 and 21), reflecting the interplay of higher-frequency eustasy with third-order eustasy. The changeover from the transgressive systems tract to the highstand systems tract is marked by a demonstrable change in cycle and megacycle stacking patterns in the platform interior of the Latemar buildup; notably, fourth-order amalgamated megacycles of the lower platform facies give way upward to fourth-order rhythmic megacycles of the lower cyclic facies (Figs. 10 and 21). Thus, the top of the lower platform facies approximates the maximum flooding surface. The highstand systems tract developed in response to a progressive decrease in third-order accommodation space (Fig. 9), primarily the result of a third-order eustatic fall (Goldhammer and Harris, 1989). This systems tract may be subdivided into an early highstand phase (the lower cyclic facies with fourth-order rhythmic megacycles) and a late highstand phase (the lower half of the tepee facies with fourth-order condensed megacycles). Within the highstand systems tract, the style and abundance of early diagenesis changes dramatically; early-marine diagenetic features are virtually absent, and subaerial exposure features are the rule. Higher-frequency cycles form an aggradational, upward-shallowing, stacking pattern as reflected by an overall thinning of fifth-order cycles and an increase in the intensity of early subaerial diagenesis (that is, thicker caliche caps to cycles and the development of subaerial tepees) from the base of the lower cyclic facies on into the tepee facies. The first Latemar sequence (sequence L1, Fig. 8) is capped by a complex 13-m-thick stratigraphic interval that occurs in the middle of the tepee facies, consisting of numerous tepee complexes vertically superimposed one atop the other, giving the appearance of one very thick tepee zone (Fig. 21). Beneath this interval, fourth-order megacycles are, overall, thinning upward; above this interval, they are, overall, thickening upward into the upper half of the tepee facies and the overlying upper cyclic facies (Fig. 21). It must be stressed, however, that *these changes are transitional*, and the thick tepee zone is not a singular erosional unconformity but is simply a zone where subaerial tepee caps on top of fifth-order subtidal cycles reached their maximum development. This interval, which records the shift from continuously decreasing to continuously increasing third-order accommodation (Fig. 9), must contain the upper sequence boundary of the first Latemar sequence (sequence L1, Fig. 8). This upper sequence boundary, which is transitional but characterized by pronounced subaerial exposure (which in detail is the superimposition of numerous higher-frequency subaerial exposure surfaces), lacks subaerial erosion and cannot be demonstrably linked downdip with any lowstand deposit in the foreslope environment. It is interpreted to have formed during the stage when third-order eustatic sea level reached its maximum rate of fall but under conditions wherein fall rate was always less than the rate of subsidence of the platform. This interpretation is substantiated by inspection of our third-order accommo-

dation-potential curve (Fig. 9; note that the rate of fall on the deviation curve, interpreted as eustasy, is less than the rate of mean subsidence). This capping boundary is thus a conformable boundary (on the scale of biostratigraphic resolution) composed of numerous closely spaced (in time, as well as in stratigraphic space) disconformities, more akin to a type 2 sequence boundary, but lacking a correlative unconformity.

Above this sequence boundary, the next Ladinian sequence (L2) is incompletely exposed, owing to Alpine erosion, but throughout the Dolomites, late Ladinian–early Carnian volcanism and tectonism terminated carbonate platform deposition. This partial sequence consists of the upper half of the tepee facies and the overlying upper cyclic facies. Thus, only the transgressive systems tract of this second Ladinian sequence is preserved at the Latemar. It is characterized by the systematic vertical shift from fourth-order condensed megacycles of the upper portion of the tepee facies to rhythmic megacycles of the upper cyclic facies (Fig. 21).

The Latemar provides a well-exposed, seismic-scale outcrop example through which sequence stratigraphy may be integrated with facies and cyclic stratigraphy. All parts of the system, from the smallest stratigraphic building block (meter-scale fifth-order cycle) to the entire third-order sequence, are observable. A critical step in the link of small cycles to big cycles is an understanding of the stacking patterns of the higher-frequency cycles, a subject that requires an appreciation of "missed beat" stratigraphy, as demonstrated by the Latemar example.

Sea-Level Changes and the Stratigraphy of Early Diagenesis

The following connections between the stratigraphy of early diagenesis of carbonate platforms and long-term changes in relative sea level were derived from our analysis of the diagenetic features of Alpine Triassic carbonates, and might have some general applicability. During a long-term increase in space for subtidal sediment accumulation, driven mainly, say, by a third-order sea-level rise, *submarine diagenesis* will dominate. Cycle thickness will be at a maximum, with bedding planes defined by widely spaced exposure surfaces or changes in subtidal lithologies. Submarine hardgrounds, reworked cemented clasts, bioerosion, and submarine tepees may develop in response to short-term slow downs or shut downs of sedimentation. Amalgamated cycles resulting from subtidal missed beats will complicate or foil the detection of high-frequency cycle rhythms. In contrast, during a long-term decrease in the accumulation space for subtidal sediments, *subaerial diagenesis* will dominate. Thin cycles capped by exposure surfaces yield very low net sedimentation rates, as considerable hiatuses are hidden at the cycle boundaries. Missing time is recorded by extensive subaerial diagenesis with several possible expressions. Humid climates will promote the development of soils with considerable karstic dissolution of subtidal sediments during short-term relative sea-level falls. Arid climate cycles will show caliche development and possibly displacive evaporite formation. Peritidal tepee formation is favored during this regime if high-frequency sea-level falls are small in amplitude, allowing for near-continuous solute supply from the shallow phreatic zone (both marine and meteoric) to promote extensive growth of tepee cores. Tepee formation is also facilitated by the ease with which previously formed thin cycles can be disrupted by expansive cementation. Meter-scale stratigraphic stacking rhythms will be disrupted and camouflaged by "missed beats" of sea level that leave no thickness record and are detectable only in the increased intensity and frequency of vadose diagenetic features.

During the periods of transition between long-term increases and long-term decreases in accumulation space (at the crests and troughs of third-order sea-level waves), meter-scale cycles defined by exposure surfaces at regular intervals come into predominance. Progradational cycles may be capped by supratidal deposits (mudcracked laminites and so on), whereas diagenetic cycles produced by relative sea-level change will be marked by caliche crusts or soils, depending on the prevailing climate during vadose diagenesis. High-frequency rhythmic sea-level oscillations, if present, have their best chance of being detected by statistical analysis of the stacking patterns of disconformity-bounded units deposited during these transitional periods.

If the magnitude of short-term tectonics or sea-level change overwhelms the long-term trends, then the resulting stratigraphic distribution of diagenetic styles will be chaotic. Styles of subaerial exposure will vary randomly, and cycles will show a wide range of thicknesses (as in the Lofer cyclothems). Faced with such a record, the best possible recourse may be to look for intervals of relative consistency in cycle thickness or cycle diagenesis in hopes of detecting short-term patterns or rhythms.

CONCLUSIONS

The Ladinian Latemar buildup preserves the most legible record of the principles governing the accumulation of Triassic carbonate platforms of the Alps, and the following conclusions are based mainly on the Latemar cyclostratigraphic record.

(1) Composite eustasy (superimposed third, fourth, and fifth order) exercised a principal control on the cyclostratigraphy and facies stratigraphy of the Triassic platform carbonates of the Alps.

(2) The short-term stacking patterns of the fifth-order depositional cycles were governed by fourth-order eustasy, producing a record of rhythmic sedimentation in tune to Milankovitch frequencies.

(3) The long-term systematic vertical changes in the stacking patterns of the high-frequency depositional cycles (fourth and fifth orders) were dictated by the low-frequency (third order) rise and fall of sea level. In particular, increase in accommodation potential on the rising limb of a third-order sea-level change resulted in thick cycles, extensive submarine diagenesis, and amalgamated megacycles due to "missed beats" of exposure, whereas decrease in accommodation potential on the falling limb of a third-order sea-level change resulted in thin cycles, extensive subaerial diagenesis, and condensed megacycles due to "missed beats" of submergence. These long-term systematic changes are independent of whether the high-frequency cycles are of allocyclic or autocyclic origin.

(4) Composite eustasy also controls the stratigraphy of early diagenesis because it regulates the timetable of subaerial exposure and submarine drowning (see 3 above).

(5) On the basis of our study of Alpine Triassic carbonates, we suggest that there exists, in general, a hierarchy of stratigraphic forcing driven by composite eustasy that controls the stratigraphic stacking patterns of depositional cycles and their early diagenesis in shallow-marine carbonates (and perhaps shallow-marine deposits of all kinds).

(6) An understanding of composite eustasy related to third-order sea-level changes and its potential for imposing a hierarchy of stratigraphic forcing provides a link between meter-scale cyclostratigraphy and kilometer-scale sequence stratigraphy.

(7) The concept of stratigraphic forcing in cyclic stratigraphy related to third-order sea-level changes has major implications for the use of the stacking patterns and characteristics of high-frequency (fourth and fifth order) depositional cycles to identify third-order depositional sequences, particularly where stratigraphic and seismic control are poor.

(8) Shallow-marine carbonate third-order sequences deposited on flat-topped platforms and banks are likely to have transitional boundaries rather than unconformable boundaries and thus would not be detected in seismic profiles. It is in these deposits that the stacking patterns of the high-frequency depositional cycles may be the only means of identifying sequences.

ACKNOWLEDGMENTS

This work is part of an ongoing project on the sedimentology and diagenesis of the Triassic carbonates of the Southern Alps, carried out in conjunction with Dr. Alfonso Bosellini of the University of Ferrara. Dr. Bosellini got us started on the study, tutored us on the geology of the Dolomites, and provided scientific advice, logistical support, and good companionship on many field trips. We gratefully acknowledge his help. We would also like to take this opportunity to acknowledge the efforts in the field and in discussions of Drs. Carlo Doglioni, Edith Newton Wilson, and Mark Harris. Linda Hinnov carried out high-resolution time-series analysis for us and schooled us in Milankovitch theory. Patrick Lehmann reviewed the manuscript and offered constructive suggestions. We thank the Gabrielli family for taking care of us in the Refugio Torre di Pisa and for other logistical assistance with our field work on the Latemar massif.

The work was funded by National Science Foundation Grants EAR85-10827 and EAR88-16638 (to L. A. Hardie) and Exxon Production Research Company (to R. K. Goldhammer and P. A. Dunn).

REFERENCES CITED

Algeo, T. J., and Wilkinson, B. H., 1988, Periodicity of mesoscale Phanerozoic sedimentary cycles and the role of Milankovitch orbital modulation: Journal of Geology, v. 96, p. 313–322.

Barrell, J., 1917, Rhythms and the measurements of geologic time: Geological Society of America Bulletin, v. 28, p. 745–904.

Beach, D. K., and Ginsburg, R. N., 1980, Facies succession of Pliocene-Pleistocene carbonates, northwestern Great Bahama Bank: American Association of Petroleum Geologists Bulletin, v. 64, p. 1634–1642.

Berger, A., 1988, Milankovitch theory and climate: Reviews of Geophysics, v. 26, p. 624–657.

Bosellini, A., 1965, Analisi petrografica della "Dolomia Principale" nel Gruppo di Sella (Regione Dolomitica): Memorie Geopaleontologiche dell'Università de Ferrara, v. 1, p. 49–109.

——1967, La tematica deposizionale della Dolomia Principale (Dolomiti e Prealpi Venete): Bollettino della Società Geologica Italiana, v. 86, p. 133–169.

——1984, Progradation geometries of carbonate platforms: Examples from the Triassic of the Dolomites, northern Italy: Sedimentology, v. 31, p. 1–24.

Bosellini, A., and Hardie, L. A., 1985, Facies e cicli della Dolomia Principale delle Alpi Venete: Memorie della Società Geologica Italiana, v. 30, p. 245–266.

Bosellini, A., and Rossi, D., 1974, Triassic carbonate buildups of the Dolomites, northern Italy: Society of Economic Paleontologists and Mineralogists Special Publication 18, p. 209–233.

Bott, M.H.P., 1982, The interior of the Earth (2nd edition): New York, Elsevier, 403 p.

Broecker, W. S., and Thurber, D. L., 1965, Uranium-series dating of corals and oolites from Bahaman and Florida Key limestones: Science, v. 149, p. 58–60.

Brown, L. F., Jr., and Fisher, W. L., 1977, Seismic-stratigraphic interpretation of depositional systems: Examples from Brazilian rift and pull-apart basins, *in* Payton, C. E., ed., Seismic stratigraphy—Applications to hydrocarbon exploration: American Association of Petroleum Geologists Memoir 26, p. 213–248.

Cisne, J. L., 1986, Earthquakes recorded stratigraphically on carbonate platforms: Nature, v. 323, p. 320–322.

Crevello, P. D., Wilson, J. L., Sarg, J. F., and Read, J. F., eds., 1989, Controls on carbonate platform and basin development: Society of Economic Paleontologists and Mineralogists Special Publication 44, 405 p.

Crowell, J. C., 1982, Continental glaciation through geologic time, *in* Berger, W. H., and Crowell, J. C., panel co-chairmen, Climate in Earth history: Washington, D.C., National Academy Press, p. 77–82.

Donovan, D. T., and Jones, E., 1979, Causes of world-wide changes in sea level: Geological Society of London Journal, v. 136, p. 187–192.

Dunn, P. A., Goldhammer, R. K., and Hardie, L. A., 1986, Mr. Sediment—A computer model for carbonate cyclicity: Geological Society of America Abstracts with Programs, v. 18, p. 590.

Eberli, G. P., and Ginsburg, R. N., 1989, Cenozoic progradation of northwestern Great Bahama Bank, a record of lateral platform growth and sea level fluctuations, *in* Crevello, P. D., and others, eds., Controls on carbonate platform and basin development: Society of Economic Paleontologists and Mineralogists Special Publication 44, p. 339–352.

Enos, P., and Perkins, R. D., 1979, Evolution of Florida Bay from island stratigraphy: Geological Society of America Bulletin, v. 90, p. 59–83.

Fischer, A. G., 1964, The Lofer cyclothems of the Alpine Triassic: Kansas Geological Survey Bulletin, v. 169, p. 107–149.

——1975, Tidal deposits, Dachstein Limestone of the North-Alpine Triassic, *in* Ginsburg, R. N., ed., Tidal deposits: New York, Springer-Verlag, p. 235–242.

——1986, Climatic rhythms recorded in strata: Annual Reviews of Earth and Planetary Sciences, v. 14, p. 351–376.

Gaetani, M., Fois, E., Jadoul, F., and Nicora, A., 1981, Nature and evolution of Middle Triassic carbonate buildups in the Dolomites (Italy): Marine Geology, v. 44, p. 25–57.

Ginsburg, R. N., 1971, Landward movement of carbonate mud: New model for regressive cycles in carbonates [abs.]: American Association of Petroleum Geologists Bulletin, v. 55, p. 340.

Goldhammer, R. K., 1987, Platform carbonate cycles, Middle Triassic of northern Italy: The interplay of local tectonics and global eustasy [Ph.D. dissert.]: Baltimore, Maryland, The Johns Hopkins University, 468 p.

Goldhammer, R. K., and Harris, M. T., 1989, Eustatic controls on the stratigraphy and geometry of the Latemar buildup (Middle Triassic), the Dolomites of northern Italy, *in* Crevello, P. D., and others, eds., Controls on carbonate platform and basin development: Society of Economic Paleontologists and Mineralogists Special Publication 44, p. 323–338.

Goldhammer, R. K., Dunn, P. A., and Hardie, L. A., 1987, High frequency glacio-eustatic sea level oscillations with Milankovitch characteristics recorded in Middle Triassic platform carbonates in northern Italy: American Journal of Science, v. 287, p. 853–892.

Grabau, A. W., 1924, Principles of stratigraphy: New York, Seiler and Co., 1,185 p.

Haas, J., 1982, Facies analysis of the cyclic Dachstein Limestone Formation (Upper Triassic) in the Bakony Mountains, Hungary: Facies, v. 6, p. 75–84.

Haq, B. U., Hardenbol, J., and Vail, P. R., 1987, Chronology of fluctuating sea levels since the Triassic: Science, v. 235, p. 1156–1167.

Hardie, L. A., 1977, Sedimentation on the modern carbonate tidal flats of northwest Andros Island, Bahamas: Baltimore, Maryland, Johns Hopkins University Press, 202 p.

——1989, Cyclic platform carbonates in the Cambro-Ordovician of the central Appalachians: International Geological Congress, 28th, Guidebook for Field Trip T161: Washington, D.C., American Geophysical Union, p. 51–81.

Hardie, L. A., and Ginsburg, R. N., 1977, Layering: The origin and environmental significance of lamination and thin bedding, *in* Hardie, L. A., ed., Sedimentation on the modern carbonate tidal flats of northwest Andros Island, Bahamas: Baltimore, Maryland, Johns Hopkins University Press, p. 50–123.

Hardie, L. A., and Shinn, E. A., 1986, Carbonate depositional environments, modern and ancient, 3, Tidal flats: Colorado School of Mines Quarterly, v. 81, no. 1, 74 p.

Hardie, L. A., Bosellini, A., and Goldhammer, R. K., 1986, Repeated subaerial exposure of subtidal carbonate platforms, Triassic, northern Italy: Evidence for high frequency sea level oscillations on a 10^4 year scale: Paleoceanography, v. 1, p. 447–457.

Harland, W. B., Cox, A. V., Llewellyn, P. G., Picton, C. A., Smith, A. G., and Walters, R., 1982, A geological time scale: New York, Cambridge University Press, 131 p.

Harris, M. T., 1988, Margin and foreslope deposits of the Latemar carbonate buildup (Middle Triassic), the Dolomites, northern Italy [Ph.D dissert.]: Baltimore, Maryland, The Johns Hopkins University, 433 p.

Harris, P. M., 1979, Facies anatomy and diagenesis of a Bahamian ooid shoal: Sedimenta VII, University of Miami Comparative Sedimentology Laboratory, 163 p.

Hays, J. D., Imbrie, J., and Shackleton, N. J., 1976, Variations in the Earth's orbit: Pacemaker of the ice ages: Science, v. 194, p. 1121–1132.

Heckel, P. H., 1986, Sea-level curve for Pennsylvanian eustatic marine transgressive-regressive depositional cycles along midcontinent outcrop belt, North America: Geology, v. 14, p. 330–334.

Hinnov, L., and Goldhammer, R. K., 1988, Identification of Milankovitch signals in Middle Triassic platform carbonate cycles using a super-resolution spectral technique [abs.]: American Association of Petroleum Geologists Bulletin, v. 72, p. 197.

House, M. R., 1985, A new approach to an absolute time scale from measurements of orbital cycles and sedimentary microrhythms: Nature, v. 315, p. 721–725.

Imbrie, J., 1985, A theoretical framework for the Pleistocene ice ages: Geological Society of London Journal, v. 142, p. 417–432.

Imbrie, J., Hays, J. D., Martinson, D. G., McIntyre, A., Mix, A. C., Morley, J. J., Pisias, N. G., Prell, W. L., and Shackleton, N. J., 1984, The orbital theory of Pleistocene climate: Support from a revised chronology of the marine $\delta^{18}O$ record, *in* Berger, A., Imbrie, J., Hays, J., Kukla, G., and Saltzman, B., eds., Milankovitch and climate: Boston, Massachusetts, Reidel, p. 269–306.

Kendall, G. St. C., and Schlager, W., 1981, Carbonates and relative changes in sea level: Marine Geology, v. 44, p. 181–212.

Land, L. S., Mackenzie, F. T., and Gould, S. J., 1967, Pleistocene history of Bermuda: Geological Society of America Bulletin, v. 78, p. 993–1006.

Miall, A. D., 1984, Principles of sedimentary basin analysis: New York, Springer-Verlag, 490 p.

Mitchum, R. M., Jr., Vail, P. R., and Thompson, S., III, 1977, Part II, The depositional sequence as a basic unit for stratigraphic analysis, *in* Payton, C. E., ed., Seismic stratigraphy—Applications to hydrocarbon exploration: American Association of Petroleum Geologists Memoir 26, p. 53–62.

Mitterer, R. M., 1975, Ages and diagenetic temperatures of Pleistocene deposits of Florida based on isoleucine epimerization in *Mercenaria*: Earth and Planetary Science Letters, v. 28, p. 275–282.

Multer, H. G., and Hoffmeister, J. E., 1968, Subaerial laminated crusts of the Florida Keys: Geological Society of America Bulletin, v. 79, p. 183–192.

Nguyen, C., Goldhammer, R. K., and Hardie, L. A., 1985, Depositional facies mosaics and their time lines in Lower Ordovician carbonates of the central Appalachians [abs.]: American Association of Petroleum Geologists Bulletin, v. 69, p. 292.

Odin, G. S., and Letolle, R., 1982, The Triassic time scale in 1981, *in* Odin, G. S., ed., Numerical dating in stratigraphy, Part 1: New York, Wiley-Interscience, p. 523–533.

Osmond, J. K., Carpenter, J. R., and Windom, H. L., 1965, $^{230}Th/^{234}U$ age of the Pleistocene corals and oolites of Florida: Journal of Geophysical Research, v. 70, p. 1843–1847.

Palmer, A. R., 1983, The Decade of North American Geology 1983 geologic time scale: Geology, v. 11, p. 503–504.

Park, J. J., and Herbert, T. D., 1987, Hunting for paleoclimatic periodicities in a geologic time series with an uncertain time scale: Journal of Geophysical Research, v. 92, p. 14027–14040.

Perkins, R. D., 1977, Depositional framework of Pleistocene rocks in south Florida: Geological Society of America Memoir 147, p. 131–198.

Pitman, W. C., 1978, Relationship between eustasy and stratigraphic sequences of passive margins: Geological Society of America Bulletin, v. 89, p. 1389–1403.

Read, J. F., and Goldhammer, R. K., 1988, Use of Fischer plots to define third-order sea-level curves in Ordovician peritidal cyclic carbonates, Appalachians: Geology, v. 16, p. 895–899.

Read, J. F., Grotzinger, J. P., Bova, J. A., and Koerschner, W. F., 1986, Models for generation of carbonate cycles: Geology, v. 14, p. 107–110.

Rona, P. A., 1973, Relations between rates of sediment accumulation on continental shelves, sea-floor spreading, and eustasy inferred from the central North Atlantic: Geological Society of America Bulletin, v. 84, p. 2851–2871.

Ruhe, R. V., Cady, J. G., and Gomez, R. S., 1961, Paleosols of Bermuda: Geological Society of America Bulletin, v. 72, p. 1121–1141.

Sander, B., 1936, Beitrage zur Kenntnis der Anlagerungsgefuge (Rhythmische Kalke und Dolomite aus der Trias): Mineralogische und Petrographische Mitteilungen, v. 48, p. 27–139.

——1951, Contributions to the study of depositional fabrics (rhythmically deposited Triassic limestones and dolomites): Tulsa, Oklahoma, American Association of Petroleum Geologists, 207 p.

Sarg, J. F., 1989, Carbonate sequence stratigraphy, *in* Wilgus, S., and others, eds., Sea level changes—An integrated approach: Society of Economic Paleontologists and Mineralogists Special Publication 43, p. 155–181.

Schlager, W., 1981, The paradox of drowned reefs and carbonate platforms: Geological Society of America Bulletin, v. 92, p. 197–211.

——1989, Drowning unconformities on carbonate platforms, *in* Crevello, P. D., and others, eds., Controls on carbonate platform and basin development: Society of Economic Paleontologists and Mineralogists Special Publication 44, p. 15–25.

Schwarzacher, W., 1954, Die grossrhythmik des Dachstein Kalkes von Lofer: Tschermaks Mineralogische und Petrographische Mitteilungen, v. 4, p. 44–54.

——1975, Sedimentation models and quantitative stratigraphy: Developments in Sedimentology 19: New York, Elsevier, 382 p.

——1987, Astronomical cycles for measuring geological time: Modern Geology, v. 11, p. 375–381.

Schwarzacher, W., and Haas, J., 1986, Comparative statistical analysis of some Hungarian and Austrian Upper Triassic peritidal carbonate sequences: Acta Geologica Hungarica, v. 29, p. 175–196.

Stanley, S. M., 1966, Paleoecology and diagenesis of Key Largo Limestone, Florida: American Association of Petroleum Geologists Bulletin, v. 50, p. 1927–1947.

Suess, E., 1888, Das Antlitz der Erder (Volume 2) (English translation "The face of the Earth" by Sollas, 1906): Oxford, United Kingdom, Clarendon Press, 556 p.

Vail, P. R., 1987, Seismic stratigraphy interpretation procedure, *in* Bally, A. W., ed., Atlas of seismic stratigraphy (Volume 1): American Association of Petroleum Geologists Studies in Geology 27, p. 1–10.

Vail, P. R., Mitchum, R. M., Jr., and Thompson, S., III, 1977, Seismic stratigraphy and global changes of sea level, Part 4: Global cycles of relative changes of sea level, *in* Payton, C. E., ed., Seismic stratigraphy—Applications to hydrocarbon exploration: American Association of Petroleum Geologists Memoir 26, p. 83–97.

Van Wagoner, J. C., Mitchum, R. M., Jr., Posamentier, H. W., and Vail, P. R., 1987, Key definitions of sequence stratigraphy, *in* Bally, A. W., ed., Atlas of seismic stratigraphy (Volume 1): American Association of Petroleum Geologists Studies in Geology 27, p. 11–14.

Webb, J. A., 1981, A radiometric time scale of the Triassic: Geological Society of Australia Journal, v. 28, p. 107–121.

Wilson, J. L., 1975, Carbonate facies in geologic history: New York, Springer-Verlag, 471 p.

MANUSCRIPT RECEIVED BY THE SOCIETY FEBRUARY 17, 1989
REVISED MANUSCRIPT RECEIVED JUNE 28, 1989
MANUSCRIPT ACCEPTED JULY 19, 1989

Printed in U.S.A.